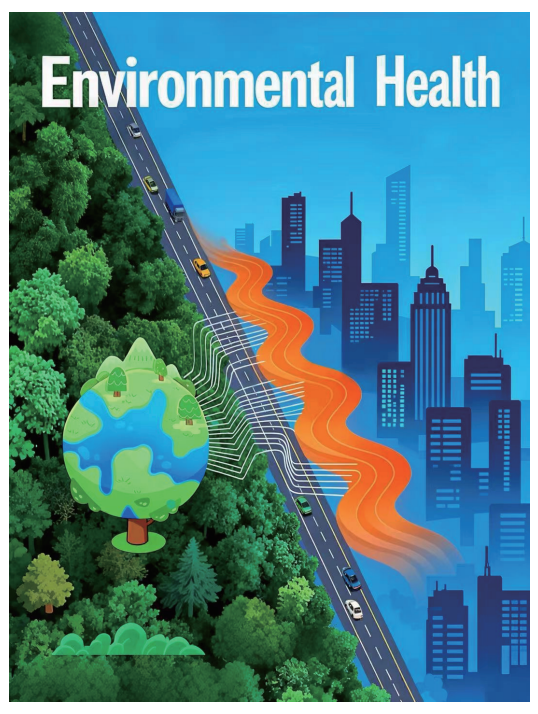
#### CHINA CDC WEEKLY

# Vol. 7 No. 45 Nov. 7, 2025 Weekly

中国疾病预防控制中心周报



#### Recollections

Reflections on the Evolution of Heat Alert Systems into Heat Health Risk Warning Systems

1409

#### **Vital Surveillances**

Individual-Level, Multi-Provincial Analysis of High Temperature and Heat-Related Illness Association — China, 2013–2022

1413

County-Level Hotspot Identification and Spatial Regression Analysis of Health Loss from Kashin– Beck Disease — China, 2019 and 2023

1418

#### **Preplanned Studies**

Development of a Landscape Pattern Health Index and Association with Stroke Mortality Using GWQS Regression — Ningbo City, Zhejiang Province, China, 2001–2023

1424







#### China CDC Weekly

#### **Editorial Board**

**Editor-in-Chief** Hongbing Shen **Founding Editor** George F. Gao

Deputy Editor-in-Chief Liming Li Gabriel M Leung Zijian Feng

**Executive Editor** Chihong Zhao **Members of the Editorial Board** 

Rui Chen Wen Chen Xi Chen (USA) Zhuo Chen (USA) Ganggiang Ding Xiaoping Dong Pei Gao Mengjie Han Yuantao Hao Na He Yuping He Guoqing Hu Zhibin Hu Yuegin Huang Na Jia Weihua Jia Zhongwei Jia Guangfu Jin Xi Jin Biao Kan Ni Li Haidong Kan Qun Li Ying Li Zhenjun Li Min Liu Qiyong Liu Xiangfeng Lu Jun Lyu Huilai Ma Jiaqi Ma Chen Mao Xiaoping Miao Ron Moolenaar (USA) Daxin Ni An Pan William W. Schluter (USA) Lance Rodewald (USA) Yiming Shao Xiaoming Shi RJ Simonds (USA) Xuemei Su Yuelong Shu Chengye Sun Quanfu Sun Feng Tan Xin Sun **Jinling Tang Huaging Wang** Hui Wang Linhong Wang Tong Wang Guizhen Wu Jing Wu Xifeng Wu (USA) Yongning Wu Min Xia Ningshao Xia Yankai Xia Lin Xiao Zundong Yin Dianke Yu Hongjie Yu Hongyan Yao Shicheng Yu Ben Zhang Jun Zhang Liubo Zhang Wenhua Zhao Yanlin Zhao Xiaoying Zheng Maigeng Zhou

Xiaonong Zhou Guihua Zhuang

#### **Advisory Board**

**Director of the Advisory Board** Jiang Lu

Vice-Director of the Advisory Board Yu Wang Jianjun Liu Jun Yan

Members of the Advisory Board

Chen Fu Gauden Galea (Malta) Dongfeng Gu Qing Gu Yan Guo Ailan Li Jiafa Liu Peilong Liu Yuanli Liu Kai Lu Roberta Ness (USA) **Guang Ning** Minghui Ren Chen Wang Hua Wang Kean Wang Xiaoqi Wang Zijun Wang Fan Wu Xianping Wu Jingjing Xi Jianguo Xu Gonghuan Yang Tilahun Yilma (USA)

Guang Zeng Xiaopeng Zeng Yonghui Zhang Bin Zou

#### **Editorial Office**

Directing Editor Chihong Zhao
Managing Editors Yu Chen
Senior Scientific Editors

Xuejun Ma Daxin Ni Ning Wang Wenwu Yin Shicheng Yu Jianzhong Zhang Qian Zhu

**Scientific Editors** 

Weihong Chen Tao Jiang Xudong Li Nankun Liu Liwei Shi Liuying Tang Meng Wang Zhihui Wang Qi Yang Qing Yue Lijie Zhang Ying Zhang

#### Recollections

#### Reflections on the Evolution of Heat Alert Systems into Heat Health Risk Warning Systems

Taiyuan Zhang<sup>1,8</sup>; Yuxin Zeng<sup>2,8</sup>; Yu Lan<sup>3</sup>; Qinghua Sun<sup>4</sup>; Pengran Qi<sup>1</sup>; Min Li<sup>1</sup>; Tiantian Li<sup>4,#</sup>

#### **ABSTRACT**

The frequent occurrence of extreme heat events in the context of global warming poses a serious threat to public health. Increasing evidence has highlighted the limitations of China's traditional early heat warning system, including an overemphasis on meteorological factors, the absence of health risk assessments, limited regional adaptability, and a disconnect between observations and public perception. shortcomings hinder the ability of the system to meet the growing demand for precise health protection and initiatives. Consequently, development of an early warning system that focuses on the health risks of high temperatures has emerged as a critical strategy for addressing climate change-related health impacts. This study systematically reviews the existing standards and service limitations of heat warning systems in China and analyzes the necessity of advancing research on and applications of healthoriented heat risk warnings. In the future, the broader social scope of such meteorological warning systems is expected to transform them into health risk assessment systems that benefit the entire population.

#### STANDARDS AND SERVICE LIMITATIONS OF HEAT WARNING SYSTEMS IN CHINA

China's meteorological departments began meteorological disaster warning operations as early as 1951. However, the modern meteorological disaster warning system, which is currently in use, was created according to the Measures for the Release and Dissemination of Meteorological Disaster Warning issued by the China Meteorological Administration (CMA) in June 2007. This regulation standardized the release and dissemination procedures for warning signals for 13 types of meteorological disasters, including typhoons, blizzards, and other severe weather events, by meteorological agencies at all administrative levels. In 2007, the National Meteorological Center formally established a national meteorological disaster warning mechanism encompassing high-temperature warnings. The latest version of the Measures for the Issuance of Meteorological Disaster Warnings in 2023 outlines 14 categories of disaster warnings that the CMA currently authorizes, clarifies the responsibilities associated with each warning, and further standardizes the operational protocols for heat alerts and the corresponding national-level response guidelines.

# Definitions of Hot Weather According to Meteorological Standards

**High temperature weather:** daily maximum temperature of  $\geq$ 35 °C (1).

**High temperature weather process:** occurrence of two or more consecutive days of hot weather (*1*).

Heat wave: a weather process with high temperature and an extended period of high humidity that causes discomfort in the human body and may pose a threat to public health and safety, along with increasing energy consumption and affecting social production activities (2).

# High-Temperature Warning Criteria of the National Meteorological Center

The National Meteorological Center issues heat alerts according to the following criteria (*3*):

Red alert: This alert is issued if parts of more than four provinces (including autonomous regions and municipalities) have experienced maximum temperatures  $\geq 40$  °C over the past 48 h, with expectations that these areas will continue to experience high temperatures  $\geq 40$  °C. Alternatively, a red alert is issued if the forecast suggests that most areas in more than four provinces (including autonomous regions and municipalities) will experience daily maximum temperatures  $\geq 40$  °C within the next 48 h.

Orange alert: This alert is issued if most areas in more than four provinces (including autonomous

regions and municipalities) have experienced daily maximum temperatures of  $\geq 37$  °C and some areas in more than two provinces have reached a temperature of  $\geq 40$  °C over the past 48 h, with expectations that these conditions will persist with temperatures remaining  $\geq 37$  °C in most areas and reaching  $\geq 40$  °C in certain regions. An orange alert is also issued if the forecast predicts that, in the next 48 h, most areas in more than four provinces (including autonomous regions and municipalities) will experience daily maximum temperatures of  $\geq 37$  °C and most areas in more than two provinces will continue to reach a temperature of  $\geq 40$  °C.

**Yellow alert:** This alert is issued if most areas in more than four provinces (including autonomous regions and municipalities) have experienced a daily maximum temperature of  $\geq 37$  °C over the past 24 h, with expectations that the hot weather in these areas will persist. A yellow alert is also issued if it is expected that most areas in more than four provinces (including autonomous regions and municipalities) will experience a daily maximum temperature of  $\geq 37$  °C over the next 48 h.

The heat alert system of the National Meteorological Center focuses not only on extreme temperatures but also on their persistence. A red alert event has occurred only once, during a widespread and prolonged heat wave in southern China from June to August 2022, with 22 consecutive warnings issued. This event affected an area of 4.53 million km² and impacted approximately 1.05 billion people. The extent of regions experiencing temperatures ≥40 °C was the largest in recorded history.

The heat alerts of the National Meteorological Center differ from those issued by provincial authorities in terms of their specific content. Furthermore, the provinces vary in terms of alert levels, issuance criteria, and regional coverage. Although the levels and wording of the warnings may vary, their primary purpose remains the same: to provide advance notice to the public to ensure that individuals can adopt appropriate precautions to mitigate the impacts of hot weather.

## LIMITATIONS OF METEOROLOGICAL HEAT ALERTS

#### **Lack of Health Risk Indicators**

Currently, heat alerts focus on meteorological features and have not yet incorporated comprehensive

health risk assessment systems. This shortcoming can be attributed to a lack of technologies that can accurately correlate meteorological conditions with health outcomes. This limitation makes it difficult to implement quantitative health risk warnings based on population characteristics and to provide targeted protection advice for high-risk groups such as older adults, individuals with chronic illnesses, and outdoor workers. This constraint affects the precision and practicality of early warnings, undermining their effectiveness in shaping public risk perceptions and responses.

#### **Lack of Regional Adaptation**

The fixed thresholds of the current warning systems cannot be adapted uniformly across regions because they fail to account for the differences in physical fitness and heat adaptation levels among residents in various areas. Therefore, health risks in atypical high-temperature regions are often underestimated. For instance, residents of northeastern China may be highly sensitive to temperatures as low as 30 °C, a threshold not adequately captured by current warning systems. Hence, the accuracy of regional adaptation and risk identification must be improved.

#### Variation Between Meteorological Observations and Real-world Perception

Although temperature observation measures in China follow international norms, temperatures are affected by complex factors in specific environments. In addition, real body temperature often differs significantly from meteorological observations. Thus, these systems do not account for the diversity in human physiological responses and health outcomes.

#### NEED FOR EARLY WARNING RESEARCH ON HIGH-TEMPERATURE HEALTH RISKS

The significant intensification of global warming and increased frequency, intensity, and duration of extreme heat events pose a significant threat to public health and social security. Heat-related deaths in China reached approximately 50,900 in 2022, representing a 342% increase compared to the historical baseline (1968–2005) (4). High temperatures can trigger heat stroke and pyrexia and significantly increase the risk of acute episodes of cardiovascular and respiratory

diseases. Therefore, establishing a heat health risk warning system is critical for improving public health preparedness and response capacity.

On July 2, 2025, the National Disease Control and Prevention Administration and CMA released the first National High Temperature Health Risk Warning, described as an "across-disciplinary collaboration between China's public health and meteorological departments in response to the frequent occurrence of extreme weather and climate events and a landmark practice to proactively address the health risks brought about by the current climate change" (5). This warning meteorological integrates data epidemiological evidence to enable a refined risk classification and region-specific management. The key features of this heat health risk warning system are as follows:

More precise risk grading: Based on relative temperature thresholds and evidence-based assessments, high-temperature health risks are classified into five levels to accommodate the diverse needs of the northern and southern regions as well as different climate zones.

More comprehensive coverage: The limitations of traditional high-temperature warnings are removed, allowing the system to include potential health risks in non-traditional high-temperature regions. This expansion helps fill the gap in heat protection systems in cold climate zones.

Service-oriented transformation and upgrading: The system has evolved from weather forecasting to issuing health-risk warnings by providing personalized health intervention recommendations for various population groups and industries. This feature marks a qualitative leap from simply "knowing the weather" to "truly knowing the people."

Health-risk warning systems are not only powerful tools for enhancing evidence-based government decision-making, but also serve as a critical foundation for medical resource allocation, public safety management, vulnerable population protection, and public health interventions. The adoption of such systems results in a significantly stronger health-emergency response capacity and improved societal resilience to climate change. Simultaneously, the widespread implementation of such early warning systems can improve public risk perception and awareness, facilitating a shift from a passive response to proactive prevention and promoting the overall health and safety of society.

# PROSPECTIVE APPLICATIONS OF HIGH-TEMPERATURE HEALTH RISK EARLY WARNINGS

In the future, while the national warning network will maintain its core function as the initiator of heat and health risk prevention and control strategies, heatrelated health risk warnings will be applied to extend beyond traditional boundaries and expand into a wide range of sectors. At the community level, integrating grid-based risk data with population characteristic databases will allow the system to support the development of a refined health management framework, enabling dynamic assessments of individual heat exposure risks and targeted interventions. In the context of clinical medical institutions, warning technology can be embedded into diagnosis and treatment decision support systems to provide a quantitative basis for risk stratification of heat-related diseases (e.g., hyperthermia and acute cardiovascular and cerebrovascular events), early screening, and optimization of intervention strategies. In the commercial sector, warning systems can offer technical support for the development of high-temperature health insurance products, provide data for demand forecasting models and supply chain optimization in ecommerce pharmaceutical enterprises, and facilitate innovation in the development of climate-adaptive products and service models for recreation and tourism industries. These applications represent comprehensive functional network of macro-level warnings, meso-level coordination, and micro-level responses. Finally, value transformation across multiple scenarios may enable meteorological early warning technologies to undergo a fundamental transformation into health warning technologies for the entire population to serve as the core infrastructure for the modernization of public health governance under the "Healthy China" initiative.

While challenges persist, such as imperfect datasharing mechanisms across industries, the need to improve cross-departmental coordinated response efficiency, and the limited adaptability of existing technologies in specific scenarios, public demand for health and safety will drive technological innovation and institutional breakthroughs. Health-weather warning technologies, exemplified by heat health risk warning systems, are expected to evolve into national health protection infrastructure, providing systematic solutions to the health challenges posed by climate

#### change.

#### Conflicts of interest: No conflicts of interest.

doi: 10.46234/ccdcw2025.236

# Corresponding author: Tiantian Li, litiantian@nieh.chinacdc.cn.

Copyright © 2025 by Chinese Center for Disease Control and Prevention. All content is distributed under a Creative Commons Attribution Non Commercial License 4.0 (CC BY-NC).

Submitted: August 27, 2025 Accepted: October 23, 2025 Issued: November 07, 2025

#### **REFERENCES**

- China Meteorological Administration. QX/T 228-2014 Classification of regional high temperature weather process. Beijing: China Meteorological Press, 2014. http://www.csres.com/detail/246195.html. (In Chinese).
- General Administration of Quality Supervision, Inspection and Quarantine of the People's Republic of China, Standardization Administration of the People's Republic of China. GB/T 29457-2012 Grade of the heat wave. Beijing: Standards Press of China, 2013. http:// www.csres.com/detail/229518.html. (In Chinese).
- China Meteorological Administration. Measures for the release of meteorological disaster warnings by the National Meteorological Center. 2023. [2025-8-6]. https://www.weather.com.cn/index/qxzs/06/628209\_ 4.shtml. (In Chinese).
- 4. Zhang SH, Zhang C, Cai WJ, Bai YQ, Callaghan M, Chang N, et al. The 2023 China report of the *Lancet* Countdown on health and climate change: taking stock for a thriving future. Lancet Public Health 2023;8 (12):e978 – 95. https://doi.org/10.1016/S2468-2667(23)00245-1.
- 5. Xu XF. Warning! Extreme heat has become a "Silent" public health killer. China Science Daily. 2025 Jul 09; Version 4. (In Chinese).

<sup>&</sup>lt;sup>1</sup> Huafeng Meteorological Media Group, China Meteorological Administration, Beijing, China; <sup>2</sup> Queen Mary College, Nanchang University, Nanchang, Jiangxi Province, China; <sup>3</sup> National Meteorological Center, Beijing, China; <sup>4</sup> National Key Laboratory of Intelligent Tracking and Forecasting for Infectious Diseases, China CDC Key Laboratory of Environment and Population Health, National Institute of Environmental Health, Chinese Center for Disease Control and Prevention, Beijing, China.

<sup>&</sup>amp; Joint first authors.

#### **Vital Surveillances**

# Individual-Level, Multi-Provincial Analysis of High Temperature and Heat-Related Illness Association — China, 2013–2022

Zhe Wang<sup>1,&,#</sup>; Runmei Ma<sup>2,&</sup>; Xiaoye Wang<sup>1</sup>; Fei Mo<sup>1</sup>; Yunzhang Zhao<sup>3</sup>; Yunxia Geng<sup>1</sup>; Yirong Liu<sup>2</sup>; Xiangxiang Wei<sup>2,4</sup>; Miao He<sup>2</sup>

#### **ABSTRACT**

Introduction Climate change is intensifying extreme heat events, positioning heat-related illness as an escalating public health threat. However, multiprovincial, individual-level evidence quantifying the association between elevated temperatures and heat-related illness in China remains limited.

Methods This multi-provincial study employed a time-stratified case-crossover design. Individual heat-related illness case data (2013–2022) were obtained from the Heat-related Illness Report System, which collects reports from local healthcare facilities and CDCs across 11 provincial-level administrative divisions (PLADs). We evaluated associations between daily mean and maximum temperatures and heat-related illness risk across multiple lag periods (lag0 to lag07), with lag01 designated a *priori* as the primary exposure window. Effect estimates are presented as relative risks (*RR*) and percentage changes in *RR* per 1°C temperature increase. Subgroup analyses examined potential effect modification by sex, age, heat-related illness subtype, heat intensity, and geographic location.

**Results** Between 2013 and 2022, 53,061 heat-related illness cases were recorded across study areas, with annual counts rising throughout the decade and reaching a peak of 14,025 in 2022. Although mild cases predominated each year (maximum 83.0% in 2015), the proportion of severe cases exhibited a concerning gradual increase. Regarding temperature associations, each 1°C increase in daily mean temperature corresponded to a 21.03% (95% *CI*: 20.59, 21.47) elevation in the *RR* of heat-related illness. Daily maximum temperature demonstrated a comparable pattern, though risk estimates were marginally lower.

**Conclusion** This study demonstrates a clear upward trend in heat-related illness incidence linked to climate change and confirms that elevated temperatures significantly increase disease risk. The escalating health burden necessitates urgent development and

implementation of targeted heat-health action plans to protect vulnerable populations.

Climate change is intensifying both the frequency and severity of heatwaves, thereby elevating risks across multiple adverse health outcomes (1), with heat-related illness emerging as a critical concern (2). Heat-related illnesses are defined as conditions resulting from prolonged exposure to high temperatures and/or strenuous physical activity in hot and humid environments, occurring when the body accumulates heat faster than its thermoregulatory capacity can dissipate it (3). These conditions have become a major public health concern during summer months. Heatrelated illnesses range from mild to severe and can be categorized into heat cramps, heat exhaustion, and heat stroke based on clinical presentation. While several local studies have documented associations between temperature and heat-related illnesses (4-6), nationallevel evidence remains limited, particularly regarding specific illness subtypes. Therefore, this study aimed to analyze the epidemiological characteristics of heatillnesses across multiple provincial-level administrative divisions (PLADs) in China from 2013 to 2022 and to quantify the association between temperature and heat-related illness risk to inform public health policy development and guide future research priorities.

Heat-related illness data spanning 2013 to 2022 were obtained from the Heat-related Illness Report System, which compiles reports submitted by local medical institutions during patient diagnosis and treatment, as well as by CDCs during the management of heat-related illness incidents (7). We focused our analysis on 11 PLADs with continuous reporting throughout the study period: Anhui, Beijing, Guangdong, Hubei, Hunan, Jiangxi, Shandong, Shanxi, Shanghai, Zhejiang, and Chongqing. Cases with missing or inconsistent patient identification

numbers or reporting addresses were excluded from the analysis. We restricted our investigation to incidents occurring between May and September, the primary heat season in China. The final analytical dataset comprised individual-level information on sex, age, reporting location, date of illness onset, and heatrelated illness subtype. Meteorological data, including hourly temperature and dewpoint temperature measurements, were retrieved from the European Weather Medium-Range (ECMWF) reanalysis database. These meteorological variables were extracted at a 0.25° spatial resolution and subsequently aggregated to generate daily countylevel metrics, including both daily mean and daily maximum values.

We employed a time-stratified case-crossover study design coupled with conditional logistic regression models, stratified by individual cases, to quantify the linear association between temperature exposure and heat-related illness risk across different subtypes. Models were adjusted for potential confounders, including daily dewpoint temperature and holiday status (categorized as weekday, weekend, or public holiday). We examined multiple exposure windows from lag0 (same-day exposure) through lag07 (7-day cumulative exposure), with lag01 (cumulative exposure over the current and previous day) designated a priori as the primary exposure window. Effect estimates were expressed as the percentage change in relative risk (RR) per 1°C increase in both mean daily temperature and maximum daily temperature. Subgroup analyses were conducted to assess effect modification by sex (male, female), age (<65 years, ≥65 years), heat-related illness subtype (mild, severe, heat cramps, heat exhaustion, heat stroke), and temperature threshold (>30 °C versus ≤30 °C for mean daily temperature; >35 °C versus ≤35 °C for maximum daily temperature). Given that Zhejiang Province contributed over 50% of all reported cases, we performed separate analyses for Zhejiang and non-Zhejiang regions to evaluate potential geographic heterogeneity in temperatureillness associations. All statistical analyses were performed using R software (version 4.4.1, R Foundation for Statistical Computing, Vienna, Austria), with statistical significance defined as P<0.05.

Between 2013 and 2022, 53,061 heat-related illness cases were documented across the study sites, demonstrating a generally upward trajectory that peaked at 14,025 cases in 2022. Geographically, Zhejiang Province accounted for the largest proportion (54.2%) of cumulative cases, followed by Anhui

(13.0%), Hubei (9.3%), Chongqing (7.7%), and Shandong (6.2%). Mild heat-related illness constituted the predominant subtype each year, reaching its highest proportion of 83.0% in 2015. Notably, severe cases exhibited a gradual proportional increase throughout the study period. Men comprised the majority of cases, with their proportion escalating to 79.5% by 2021. The age distribution remained relatively consistent, primarily affecting young and middle-aged adults, although the proportion of older individuals (≥65 years) peaked at approximately 30% in 2022 (Figure 1).

Our analysis demonstrated that each 1°C increase in daily average temperature corresponded to a 21.03% elevation in the RR of heat-related illnesses [95%] confidence interval (CI): 20.59%, 21.47%]. Stratified by population group, the RR increased by 22.03% (95% CI: 21.48%, 22.60%) for men, 26.62% (95% CI: 25.67%, 27.58%) for women, 35.67% (95% CI: 34.43%, 36.91%) for older adults, and 20.48% (95% CI: 19.96%, 21.00%) for younger individuals. All differences achieved statistical significance (P<0.05). When examining the effects of elevated temperatures, no substantial risk emerged below 30 °C. We further analyzed the relationship between temperature and specific subtypes of heat-related illness. Each 1°C increase in daily average temperature was associated with a 19.19% (95% CI: 18.66%, 19.72%) increase in mild heat-related illnesses, a 38.94% (95% CI: 37.77%, 40.13%) increase in severe heat-related illnesses, a 36.00% (95% CI: 33.90%, 38.14%) increase in heat cramps, an 86.87% (95% CI: 79.45%, 94.59%) increase in heat exhaustion, and a 62.48% (95% CI: 60.01%, 64.98%) increase in heat stroke. Daily maximum temperature exhibited a similar pattern, although the overall risk estimates were marginally lower (Figure 2). The robustness of these findings across different lag periods is presented in the Supplementary Material (Supplementary Table S1, available at https://weekly.chinacdc.cn/). Additional comparative analysis between Zhejiang and non-Zhejiang regions revealed that results based on all study sites aligned closely with those from Zhejiang Province alone, whereas findings from non-Zhejiang regions generally showed slightly higher risk estimates than those observed in Zhejiang (Supplementary Table S2, available at https://weekly.chinacdc.cn/).

#### **DISCUSSION**

This study utilized decade-long, cross-provincial

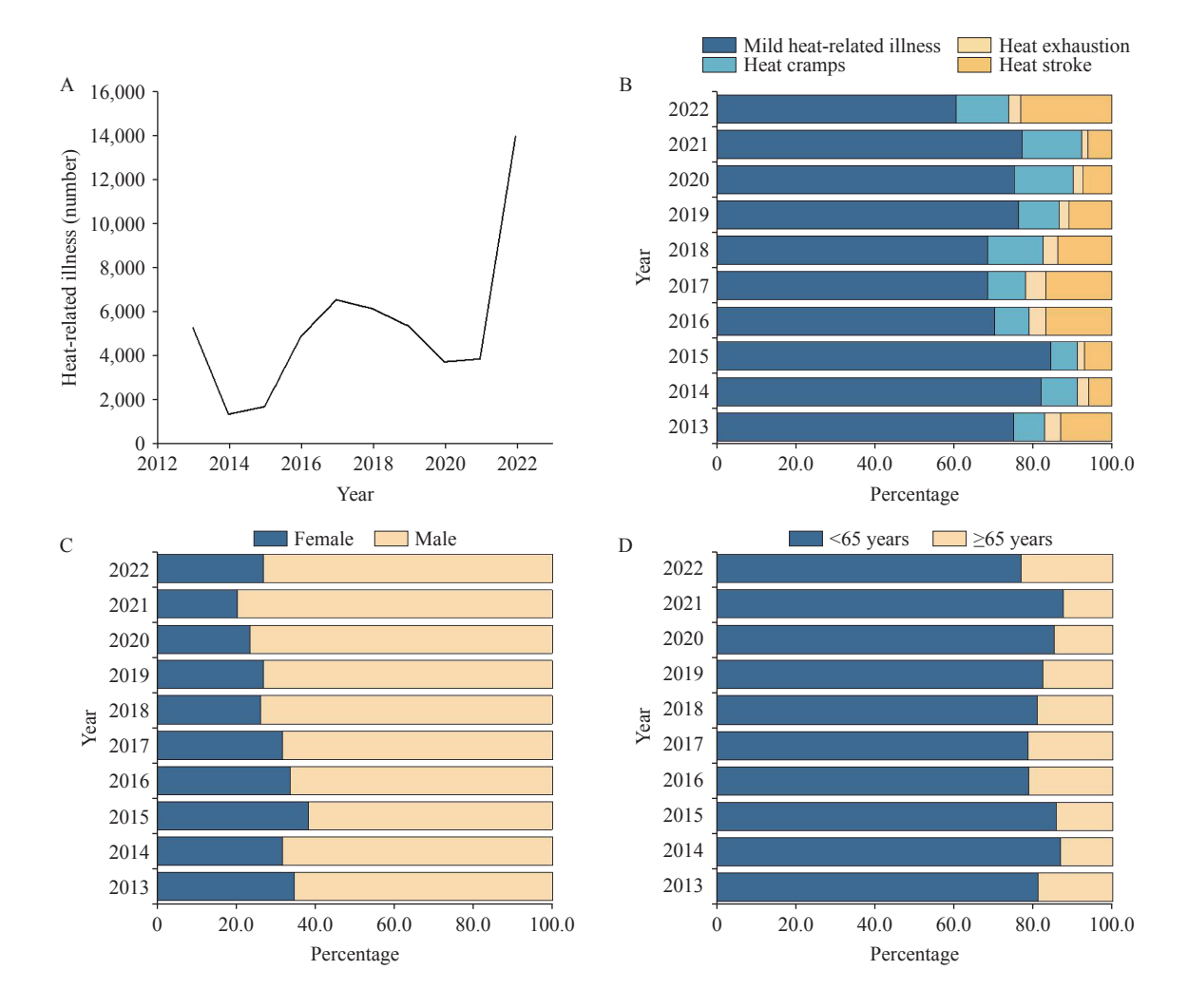


FIGURE 1. Basic characteristics of heat-related illness cases from 2013 to 2022.

(A) The annual number of heat-related illness cases; (B) The yearly distribution of heat-related illness subtypes (mild heat-related illness, severe heat-related illness, heat cramps and heat exhaustion, heat stroke); (C) The annual sex-based distribution (male, female) of heat-related illness; (D) The yearly age-based distribution (<65 years, ≥65 years) of heat-related illness.

data to characterize the spatial-temporal patterns of heat-related illness and quantify its association with temperature. Our findings reveal a generally increasing trend in heat-related illnesses over the past decade, with most cases occurring in men and individuals under 65 years of age, predominantly classified as mild heat-related illness. Notably, women and older individuals exhibited heightened sensitivity to elevated temperatures, with significant risks emerging when daily average temperatures exceeded 30°C and daily maximum temperatures surpassed 35°C. The risk of severe heat-related illness, including heat exhaustion and heat stroke, was highest under these conditions.

Our findings confirmed that high temperatures substantially increase the risk of heat-related illness, with effects persisting for several days following exposure. These results align with previous studies

(4–6), underscoring the critical importance of implementing preventive measures during extreme heat events. Without prompt recognition and treatment, heat-related illness can progress to multi-organ dysfunction, failure, and death. Given the severity of these outcomes, prevention strategies are paramount. Evidence-based protective measures during extreme heat include maintaining access to air-conditioned environments, utilizing cooling devices, ensuring adequate hydration, and minimizing strenuous physical activity (8).

Our results indicate that while men and individuals under 65 years experience a higher incidence of heat-related illnesses, likely attributable to occupational exposures and activity patterns (9), women and older adults face disproportionately greater health risks from elevated temperatures. Current studies offer varying

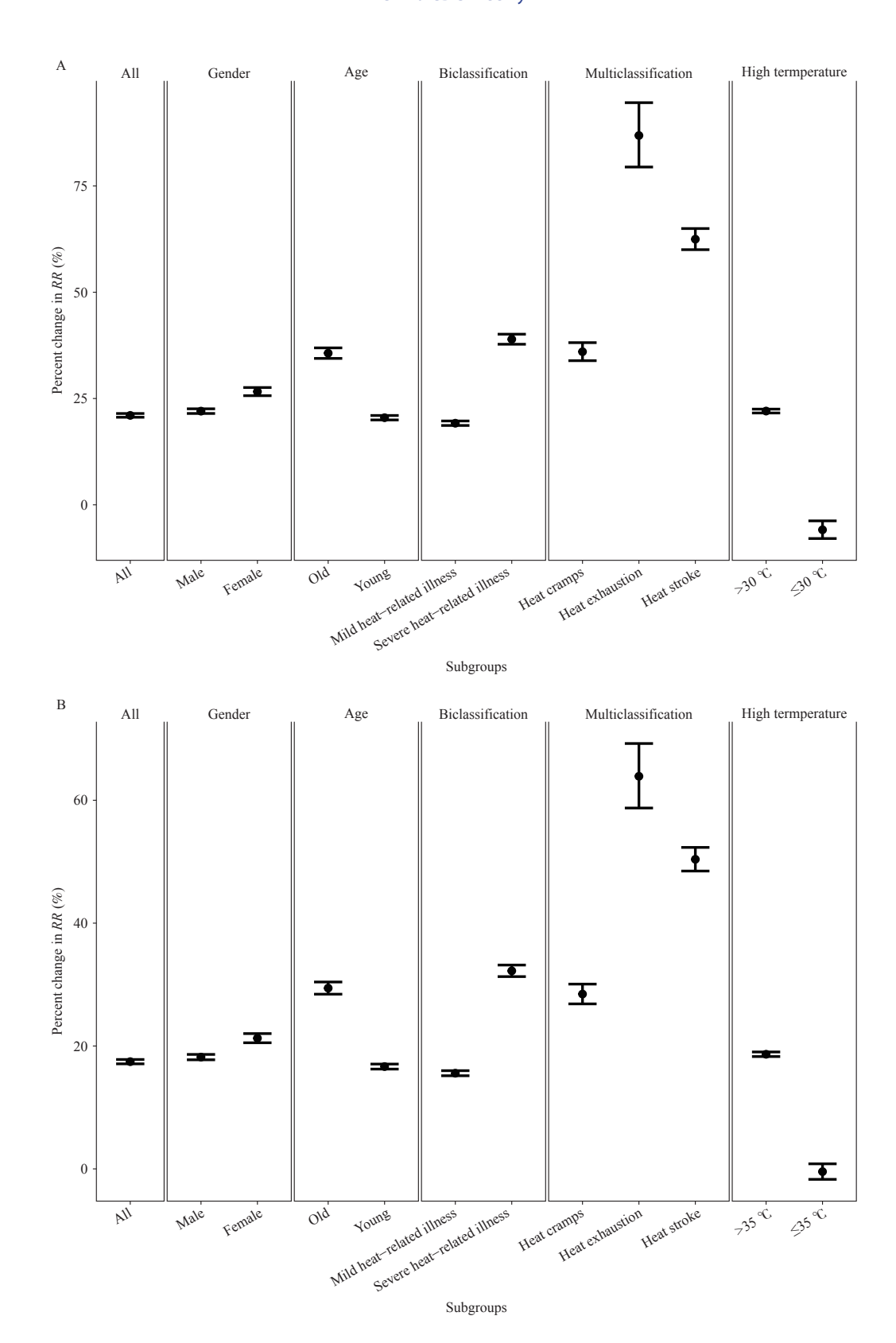


FIGURE 2. Association between temperature and heat-related illness at lag01. (A) The relationship between daily mean temperature and heat-related illness at lag01. (B) The relationship between daily maximum temperature and heat-related illness at lag01.

Note: In each graph, panels from left to right correspond to overall results, gender-stratified results, age-stratified results, subtype-stratified results, and temperature-stratified results.

Abbreviation: RR=risk ratio.

conclusions on sex differences in heat-related illness explanations susceptibility, with encompassing physiological factors, pathophysiological mechanisms, and differential exercise-heat exposure scenarios (10). Additionally, older adults demonstrate increased vulnerability to heat-related illnesses due to diminished thermoregulatory capacity and higher prevalence of chronic comorbidities (11-12). These findings highlight a critical distinction: although males and younger individuals (under 65 years) account for the majority of reported cases, females and older adults (> 65 years) exhibit greater physiological vulnerability when exposed to rising temperatures, warranting targeted protective interventions for these populations.

This study has several limitations that warrant consideration. First, the heat-related illness data relied on hospital-based reporting, meaning that not all cases were captured. Some individuals may not seek medical care, and reporting compliance varied across hospitals and local CDCs due to differences in awareness and interest in surveillance activities. Consequently, the current heat-related illness surveillance system may not accurately reflect the true disease burden in certain regions. Second, meteorological data were aggregated at the county level, which may introduce exposure misclassification at the individual level, potentially attenuating the observed temperature-health associations.

Despite these limitations, our findings carry important practical implications for public health policy and practice. It is essential to strengthen preventive measures, enhance public awareness campaigns, and improve emergency response capacity in high-risk PLADs such as Zhejiang, Jiangsu, and Anhui, with particular focus on vulnerable populations including women and older adults. Although most heat-related illnesses in our dataset were mild, likely reflecting prompt recognition and clinical intervention, the risk of severe outcomes such as heat exhaustion and heat stroke remains substantial during extreme heat Implementing comprehensive preventive strategies and ensuring timely access to medical care are critical for reducing morbidity and mortality. Furthermore, local health systems should enhance case reporting procedures to enable early detection of heatrelated illness clusters and public health emergencies. Such improvements would facilitate rapid deployment of targeted interventions in affected regions and ultimately reduce the population-level health burden associated with extreme heat exposure.

Conflicts of interest: No conflicts of interest.

**Funding:** Supported by the Major Project of Guangzhou National Laboratory (No. GZNL2024A01025) and the National Natural Science Foundation of China (Grant No. 52272340).

doi: 10.46234/ccdcw2025.238

Copyright © 2025 by Chinese Center for Disease Control and Prevention. All content is distributed under a Creative Commons Attribution Non Commercial License 4.0 (CC BY-NC).

Submitted: July 08, 2025 Accepted: October 24, 2025 Issued: November 07, 2025

#### **REFERENCES**

- Zhong Y, Chen C, Wang Q, Li TT. High temperature and risk of cause-specific mortality in China, 2013–2018. China CDC Wkly 2020;2(23):408 – 12. https://doi.org/10.46234/ccdcw2020.105.
- Romanello M, McGushin A, Di Napoli C, Drummond P, Hughes N, Jamart L. The 2021 report of the *Lancet* Countdown on health and climate change: code red for a healthy future. Lancet 2021;398(10311): 1619 – 62. https://doi.org/10.1016/S0140-6736(21)01787-6.
- Armed Forces Health Surveillance Branch. Update: heat illness, active component, U.S. Armed Forces, 2020. MSMR 2021;28(4):10-5. https://pubmed.ncbi.nlm.nih.gov/33975435/.
- Cui YX, Cui LL, Peng XM, Wang R, Zhang YJ, Li XW, et al. Relationship between hot weather and heat stroke in Ji'nan during 2011-2016. J Environ Health 2018;35(4):319 – 22. https://doi.org/10. 16241/j.cnki.1001-5914.2018.04.010.
- Li YH, Li CC, Luo SQ, He JY, Cheng YB, Jin YL. Impacts of extremely high temperature and heatwave on heatstroke in Chongqing, China. Environ Sci Pollut Res 2017;24(9):8534 – 40. https://doi.org/10.1007/ s11356-017-8457-z.
- Lu WH, Gu SH, Sun SQ, Zhang CM, Zhu XC. Quantitative analysis
  of the lagged effects of heat-wave on heatstroke in Ningbo from 2013 to
  2019. J Meteor Environ 2022;38(1):106 12. https://doi.org/10.3969/
  j.issn.1673-503X.2022.01.014.
- 7. National Health Commission of the People's Republic of China. Health emergency response plan for heatstroke incidents. 2007. https://www.nhc.gov.cn/wjw/gfxwj/200708/50ab7ed38d6a49de9c73a356b65714d2.shtml. (In Chinese).
- 8. Epstein Y, Yanovich R. Heatstroke. New Engl J Med 2019;380(25): 2449 59. https://doi.org/10.1056/NEJMra1810762.
- Asmara IGY. Diagnosis and management of heatstroke. Acta Med Indones 2020;52(1):90-7. https://pubmed.ncbi.nlm.nih.gov/32291378/.
- Giersch GEW, Garcia CK, Stachenfeld NS, Charkoudian N. Are there sex differences in risk for exertional heat stroke? A translational approach. Exp Physiol 2022;107(10):1136 – 43. https://doi.org/10. 1113/EP090402.
- Kjellstrom T, Holmer I, Lemke B. Workplace heat stress, health and productivity - an increasing challenge for low and middle-income countries during climate change. Glob Health Action 2009;2(1):2047. https://doi.org/10.3402/gha.v2i0.2047.
- Hopp S, Dominici F, Bobb JF. Medical diagnoses of heat wave-related hospital admissions in older adults. Prev Med 2018;110:81 – 5. https:// doi.org/10.1016/j.ypmed.2018.02.001.

<sup>#</sup> Corresponding author: Zhe Wang, wangzhe@chinacdc.cn.

<sup>&</sup>lt;sup>1</sup> Chinese Center for Disease Control and Prevention, Beijing, China;
<sup>2</sup> National Institute of Environmental Health, Chinese Center for Disease Control and Prevention, Beijing, China;
<sup>3</sup> National Institute for Occupational Health and Poison Control, Chinese Center for Disease Control and Prevention, Beijing, China;
<sup>4</sup> School of Public Health, Nanjing Medical University, Nanjing City, Jiangsu Province, China.

<sup>&</sup>amp; Joint first authors.

#### **SUPPLEMENTARY MATERIAL**

SUPPLEMENTARY TABLE S1. Associations between high temperature and heat-related illnesses across different lag periods.

Exposure	Model	Lag0 (%)	Lag01 (%)	Lag02 (%)	
	All	20.9 (20.47–21.34)	21.03 (20.59–21.47)	19.58 (19.14–20.01)	
	Sex				
	Male	22.17 (21.63–22.72)	22.03 (21.48–22.58)	20.05 (19.51–20.59)	
	Female	25.28 (24.36–26.21)	26.62 (25.67–27.58)	26.4 (25.43–27.37)	
	Age				
	Older	32.91 (31.74–34.09)	35.67 (34.43–36.91)	35.87 (34.62–37.14)	
	Younger	20.72 (20.21–21.24)	20.48 (19.96–21.01)	18.61 (18.09–19.13)	
	Heat intensity				
Daily mean temperature	>30 °C	21.89 (21.45–22.34)	22.05 (21.59–22.51)	20.51 (20.06–20.96)	
Jany mountompolaters	≤30 °C	-2.48 (-4.4 to -0.52)	-5.88 (-7.94 to -3.78)	-7.27 (-9.43 to -5.05)	
	Subtype				
	Mild	19.23 (18.72–19.75)	19.19 (18.66–19.71)	17.84 (17.31–18.37)	
	Severe	37.26 (36.12–38.41)	38.94 (37.77–40.13)	36.54 (35.39–37.69)	
	Heat cramps	37.11 (35.02–39.23)	36.01 (33.9–38.14)	30.53 (28.52–32.56)	
	Heat exhaustion	77.6 (70.92–84.54)	86.87 (79.45–94.59)	85.55 (78.19–93.22)	
	Heat stroke	54.97 (52.76–57.21)	62.48 (60.01–64.98)	63.23 (60.71–65.78)	
	All	17.28 (16.93–17.62)	17.45 (17.1–17.81)	16.15 (15.8–16.5)	
	Sex				
	Male	18.27 (17.84–18.7)	18.19 (17.76–18.63)	16.41 (15.98–16.84)	
	Female	20.08 (19.37–20.8)	21.27 (20.53–22.02)	21.14 (20.39–21.9)	
	Age				
	Older	27.12 (26.19–28.07)	29.43 (28.44–30.42)	29.54 (28.54–30.55)	
	Younger	16.78 (16.38–17.18)	16.65 (16.24–17.06)	15.04 (14.64–15.45)	
<b>5</b>	Heat intensity				
Daily maximum temperature	>35 °C	18.45 (18.08–18.82)	18.66 (18.28–19.03)	17.32 (16.95–17.69)	
	≤35 °C	1.85 (0.68–3.03)	-0.45 (-1.7-0.83)	-2.72 (-4.03 to -1.38)	
	Subtype				
	Mild	15.51 (15.11–15.92)	15.57 (15.16–15.99)	14.45 (14.04–14.87)	
	Severe	30.98 (30.07–31.89)	32.24 (31.3–33.18)	29.83 (28.93–30.75)	
	Heat cramps	29.8 (28.19–31.42)	28.46 (26.86–30.08)	23.33 (21.82–24.86)	
	Heat exhaustion	58.22 (53.47–63.13)	63.9 (58.74–69.24)	62.68 (57.54–67.99)	
	Heat stroke	44.35 (42.63–46.1)	50.39 (48.48–52.33)	50.86 (48.91–52.82)	

#### China CDC Weekly

SUPPLEMENTARY TABLE S2. Stratified analysis results comparing Zhejiang Province and other regions at lag01.

Exposure	Model	Lag01 of Zhejiang (%)	Lag01 of other regions (%)		
	All	22.85 (21.99–23.71)	45.74 (44.31–47.18)		
	Sex				
	Male	26.7 (25.54–27.88)	47.82 (45.99–49.67)		
	Female	27.26 (25.56–28.97)	69.85 (65.98–73.82)		
	Age				
	Older	37.56 (34.87–40.29)	82.66 (78.21–87.23)		
	Younger	23.64 (22.65–24.63)	44.31 (42.57–46.08)		
Daily maan tamparatura	Heat intensity				
Daily mean temperature	>30 °C	25.47 (24.54–26.4)	47.73 (46.23–49.24)		
	≤30 °C	-5.05 (-7.75 to -2.27)	14.41 (9.46–19.57)		
	Subtype				
	Mild	21.71 (20.77–22.65)	44.65 (42.73–46.6)		
	Severe	57.96 (54.09–61.92)	72.61 (69.25–76.03)		
	Heat cramps	52.17 (46.05–58.54)	60.78 (54.75–67.05)		
	Heat exhaustion	90.34 (73.49–108.83)	128.77 (112.24–146.59)		
	Heat stroke	77.02 (69.57–84.81)	106.69 (99.87–113.74)		
	All	17.07 (16.45–17.7)	36.49 (35.42–37.56)		
	Sex				
	Male	19.76 (18.92–20.61)	37.67 (36.32–39.04)		
	Female	19.7 (18.49–20.93)	53.49 (50.72–56.31)		
	Age				
	Older	27.12 (25.21–29.06)	63.82 (60.64–67.08)		
	Younger	17.61 (16.89–18.33)	34.78 (33.48–36.08)		
Daily maximum tomporaturo	Heat intensity				
Daily maximum temperature	>35 °C	19.27 (18.57–19.98)	39.71 (38.54–40.89)		
	≤35 °C	0.69 (-0.97 to 2.37)	12.62 (9.95–15.36)		
	Subtype				
	Mild	16.16 (15.48–16.85)	35.33 (33.89–36.78)		
	Severe	41.73 (39.02–44.5)	54.35 (52.03–56.72)		
	Heat cramps	36.7 (32.53–40.99)	45.08 (40.85–49.44)		
	Heat exhaustion	61.66 (50.57–73.58)	89.69 (79.15–100.84)		
	Heat stroke	54.85 (49.72–60.15)	77.67 (73.09–82.38)		

#### **Vital Surveillances**

#### County-Level Hotspot Identification and Spatial Regression Analysis of Health Loss from Kashin-Beck Disease — China, 2019 and 2023

Ying Liu<sup>1,2</sup>; Fang Qi<sup>1,2</sup>; Haoyu Du<sup>1,2</sup>; Haonan Li<sup>1,2</sup>; Shicong Zheng<sup>1,2</sup>; Qian Yu<sup>1,2</sup>; Hexuan Dong<sup>1,2</sup>; Chenxi Wang<sup>1,2</sup>; Jiaxin Li<sup>1,2</sup>; Yue Zhao<sup>1,2</sup>; Jiayuan Li<sup>1,2</sup>; Jun Yu<sup>1,2,#</sup>

#### **ABSTRACT**

Introduction: We analyzed the spatial distribution of years lived with disability (YLDs) among patients with Kashin–Beck disease (KBD) at the county level across the country, identified hotspot regions and the primary areas of disease burden. This provides a foundation for the prevention and control of KBD and the rational allocation of healthcare resources to regions with high disease burden.

Methods: The data were obtained from the National KBD Surveillance System. Spatial autocorrelation analysis was conducted to assess spatial clustering and to identify hotspots of YLDs in patients with KBD. Geographically weighted regression (GWR) models were used to identify counties with limited economic and healthcare resources and a high burden of health losses.

Results: Spatial aggregation of YLDs among patients with KBD was observed nationwide, with hotspots concentrated in diseased counties in western China, including Shaanxi, Gansu, and Sichuan, and in the northern regions of Heilongjiang and Inner Mongolia. Among the variables, the number of health technicians was negatively correlated with the YLD rate of patients with KBD across 2 years (*P*<0.05). Significant geographical differences were found in the spatial distribution of YLDs, with key disease burden areas in 85 northern counties, including Heilongjiang, Jilin, and Inner Mongolia, and 145 western counties, including Shaanxi, Shanxi, and other provincial-level administrative divisions.

Conclusions: YLDs among patients with KBD at the county level in China demonstrated spatial clustering, with hotspots primarily in the western regions. Strengthening the recruitment and training of health professionals in high-burden, underserved areas may help improve the quality of life of patients.

Kashin-Beck disease (KBD) is an endemic chronic osteoarticular disorder primarily affecting children (1). It is characterized by joint pain, limb deformities, shortened extremities, and growth retardation, often causing lifelong disability and reduced quality of life (2). KBD has historically been endemic to 379 counties across 13 provincial-level administrative divisions (PLADs) in China, largely along the northeast-to-southwest belt. Comprehensive interventions, including water and grain substitution, socioeconomic development, and improved healthcare, have caused its elimination and zero incidence (3-4). Nevertheless, a substantial number of individuals live with KBD and experience a significantly lower quality of life (5). However, targeted health interventions for these patients are not sufficiently supported by scientific evidence.

Currently, spatial epidemiological research on KBD is largely limited to individual PLADs or counties and lacks high-resolution county-level data at the national scale. This gap limits the effectiveness of the prevention and control strategies. Therefore, we conducted a spatial analysis of years lived with disability (YLDs) among patients with KBD across China's counties to assess spatial distribution patterns, identify high-burden areas, provide a theoretical basis for improving patient outcomes, optimizing healthcare resource allocation, and informing targeted prevention and control policies.

#### **METHODS**

The data for this study were sourced from the National KBD Surveillance System and the National Case Surveys conducted in 2019 and 2023 (6). The system conducts epidemiological surveys in KBD-endemic regions using active case-finding methods,

including household visits and physical examinations. It identifies individuals based on KBD diagnostic criteria (WS/T 207-2010), which include clinically diagnosed and imaging-confirmed cases. The dataset included the demographic information of the respondents, such as sex, age, occupation, place of residence, and disease severity. The per capita gross domestic product (GDP) was extracted from the China County Statistical Yearbook, and per capita income was derived from the same surveillance system. Data on the number of hospital beds and healthcare technicians were obtained from the National Bureau of Statistics of China. Missing values in county-level economic and healthcare indicators were addressed through multiple imputations by chained equations (MICE) (7). Specifically, this method preserves the inherent variability of the original data and, consequently, improves the accuracy and statistical efficiency of regression estimates.

We used YLDs to assess the loss of healthy life expectancy in patients with KBD due to the non-lethal nature of KBD. This measure effectively reflects the burden of non-fatal disability caused by different severities of KBD at both the individual and societal levels (8).

The YLD was calculated as follows:

#### $YLD = N \times DW$ ,

where *N* represents the number of patients with KBD and *DW* denotes the disability weight. Because previous studies have not reported the disability weights for KBD and its clinical manifestations resemble those of rheumatoid arthritis (*9*), disability weights for rheumatoid arthritis from the Global Burden of Disease (GBD) 2019 study were used as proxies for KBD. These values were 0.117, 0.317, and 0.581 for degrees I, II, and III, respectively (*10*).

The ArcGIS software (version 10.8; ESRI, California, USA) was used to assess the overall spatial aggregation of YLDs among patients with KBD using global spatial autocorrelation, whereas the Getis-Ord Gi\* statistic was employed to identify local hotspots (11). The ordinary least squares (OLS) model was used to initially examine the relationships between per capita gross domestic product (GDP), per capita income, number of hospital beds, number of health technicians, and the YLD rate among patients with KBD. Multicollinearity was assessed using the variance inflation factor (VIF), with VIF values of <10 indicating acceptable collinearity. Subsequently, a geographically weighted regression (GWR) model was

used to conduct localized estimations, revealing spatial non-stationarity in the relationships between each variable and the YLD rate across endemic areas and counties. These patterns were visualized using local regression coefficients. Key areas for disease management and priority interventions in adult patients with KBD have been identified (12–13).

#### **RESULTS**

#### **General KBD Characteristics**

KBD is endemic to 13 Chinese PLADs. Data during the first national surveillance in 2019 were collected from 325 endemic counties, reporting 164,914 prevalent cases, including 105,142 degree I, 46,702 degree II, and 13,070 degree III cases. By 2023, data collected from 379 endemic counties indicated 165,348 prevalent cases, including 103,969 degree I, 49,796 degree II, and 11,583 degree III cases.

## Spatial Distribution of YLDs in Patients with KBD

Significant regional differences were observed in the YLD rates and the YLDs of KBD in 2019 and 2023. The regions with severe loss of healthy life expectancy in 2019 were the disease area counties of Yantang County (497.87 YLD/10,000, 2,074.54 YLDs) and Aba County (289.53 YLD/10,000, 1,604.27 YLDs), both are in Sichuan Province. By 2023, the regions with severe losses were Heshui County (86.02 YLD/10,000, 1,621.58 YLDs) and Ning County (44.68 YLD/10,000, 1,367.49) in Gansu Province.

Moran's I indices for KBD-related YLDs and YLD rates were 0.11 and 0.07, respectively, in 2019, and 0.17 and 0.08, respectively, in 2023, with *P*<0.05 in both years. These results indicate significant spatial clustering of KBD-related health losses at the county level nationwide (Supplementary Figure S1, available at https://weekly.chinacdc.cn/).

The Getis-Ord-Gi\* statistic was applied to further identify hotspots. In 2019, the hotspot areas of YLD among patients with KBD were primarily concentrated in the central and western regions of China, covering 155 endemic counties across PLADs, including Henan, Shaanxi, Qinghai, Gansu, Sichuan, and Shanxi (Table 1). The hotspot areas had shifted by 2023, with concentrations in both the western and northern regions of China spanning PLADs such as Shaanxi, Qinghai, Gansu, Sichuan, Inner Mongolia, and Heilongjiang and comprising 90 endemic counties

TABLE 1. Hotspot areas of KBD YLDs rates at the county level in 2019 identified by local Getis-Ord Gi' analysis.

Hotspot type	PLADs	Counties
Hotspot: 99% confidence	Gansu Henan	Qinzhou District, Maiji District, Qingshui County, Qin'an County, Wushan County, Zhangjiachuan Hui Autonomous County, Kongtong District, Jingchuan County, Lingtai County, Chongxin County, Zhuanglang County, Huating City, Xifeng District, Qingcheng County, Huan County, Huachi County, Heshui County, Zhengning County, Ning County, Zhenyuan County, Longxi County, Weiyuan County, Zhang County, Min County, Wudu District, Cheng County, Wen County, Dangchang County, Kang County, Xihe County, Li County, Hui County, Liangdang County, Kangle County, Hezheng County, Zhuoni County, Luqu County Shanzhou District, Lushi County, Lingbao City
	Qinghai	Guide County, Xinghai County, Banma County
	Shaanxi	Baqiao District, Lintong District, Lantian County, Zhouzhi County, Wangyi District, Yintai District, Yaozhou District, Yijun County, Weibin District, Jintai District, Chencang District, Fengxiang County, Qishan County, Fufeng County, Mei County, Long County, Qianyang County, Linyou County, Feng County, Taibai County, Sanyuan County, Jingyang County, Qian County, Liquan County, Yongshou County, Changwu County, Xunyi County, Chunhua County, Binzhou City, Linwei District, Huazhou District, Tongguan County, Heyang County, Chengcheng County, Pucheng County, Baishui County, Fuping County, Hancheng City, Baota District, Ansai District, Zhidan County, Ganquan County, Fu County, Luochuan County, Yichuan County, Huanglong County, Huangling County, Nanzheng District, Xixiang County, Mian County, Ningqiang County, Lueyang County, Hanbin District, Shiquan County, Ningshan County, Shangzhou District, Luonan County, Zhen'an County, Zhashui County JiShan County, Pinglu County, Ruicheng County
	Sichuan	Beichuan Qiang Autonomous County, Pingwu County, Jiangyou City, Wangcang County, Qingchuan County, Dazhu County, Yucheng District, Hanyuan County, Shimian County, Tianquan County, Tongjiang County, Nanjiang County, Maerkang City, Wenchuan County, Mao County, Songpan County Jiuzhaigou County, Jinchuan County, Xiaojin County, Heishui County, Rangtang County, Aba County, Ruo'ergai County, Hongyuan County, Luding County, Danba County, Daofu County, Ganzi County, Xinlong County, Dege County, Seda County, Mianning County
Hotspot: 95% confidence	Henan	Luoning County, Mianchi County
Connuciac	Inner Mongolia Shanxi Shaanxi	Uxin Banner  Wanrong County, Wenxi County, Jiang County, Yuanqu County, Xia County, Xiangfen County, Ji County, Xiangning County, Daning County, Yonghe County Yanchang County
Hotspot: 90% confidence	Shanxi	Xi County, Pu County, Shilou County
COMMUNICATION	Shaanxi	Yuyang District

Abbreviation: KBD=Kashin-Beck disease; YLDs=years lived with disability; PLAD=provincial-level administrative division.

(Table 2).

#### Spatial Regression Analysis of YLDs in Patients with KBD

The data were standardized to eliminate the effects of different units and magnitudes among the variables. An OLS model was used to assess the association between the YLD rate of patients with KBD and the different factors socioeconomic globally. All independent variables had VIF values less than 10, indicating acceptable levels of multicollinearity. In 2019, the YLD rates of patients with KBD were positively associated with per capita GDP, per capita income, and the number of hospital beds, although none of these associations were statistically significant. In 2023, the YLD rates were negatively associated with per capita GDP, the number of hospital beds, and

positively associated with per capita income, with none of these associations reaching statistical significance. Furthermore, a significant negative association (P<0.05) was observed between the number of health technicians and YLD rates in both 2019 and 2023 (Table 3).

We used corrected Akaike information criterion (AICc) as the model selection metric to apply the GWR model that yielded AICc values of 769.14 and 845.17 in 2019 and 2023, respectively, whereas the OLS model produced values of 859.77 and 863.15, respectively. Thus, the GWR model provided a better fit for both years.

The GWR parameter estimation results revealed varying coefficients across different counties, further confirming the spatial heterogeneity in the determinants of YLD rates for KBD (Table 3). The OLS model results demonstrated that the number of

TABLE 2. Hotspot areas of KBD YLDs rates at the county level in 2023 identified by local Getis-Ord Gi analysis

Hotspot type	PLADs	Counties
Hotspot: 99% confidence	Gansu	Qinzhou District, Qin'an County, Wushan County, Longxi County, Weiyuan County, Zhang County, Min County, Wudu District, Cheng County, Wen County, Dangchang County, Kang County, Xihe County, Li County, Hui County, Kangle County, Hezheng County, Zhuoni County, Luqu County
	Inner Mongolia	Morin Dawa Daur Autonomous Banner
	Qinghai	Guide County, Xinghai County, Banma County
	Shaanxi	Nanzheng District, Ningqiang County, Lueyang County
	Sichuan	Beichuan Qiang Autonomous County, Pingwu County, Jiangyou City, Wangcang County, Qingchuan County, Yucheng District, Hanyuan County, Shimian County, Tianquan County, Maerkang City, Wenchuan County, Lixian County, Mao County, Songpan County, Jiuzhaigou County, Jinchuan County, Xiaojin County, Heishui County, Rangtang County, Aba County, Ruo'ergai County, Hongyuan County, Luding County, Danba County, Daofu County, Ganzi County, Xinlong County, Dege County, Seda County, Mianning County
	Xizang	Jiangda County, Gongjue County
Hotspot: 95% confidence	Gansu	Maiji District, Qingshui County, Zhangjiachuan Hui Autonomous County, Zhuanglang County, Liangdar County
	Heilongjiang	Nenjiang City, Mohe City, Huma County, Tahe County
	Inner Mongolia	Arun Banner, Eerguna City, Genhe City
	Shaanxi	Feng County, Xixiang County, Mian County
	Sichuan	Tongjiang County, Nanjiang County
	Xizang	Chaya County, Mangkang County
Hotspot: 90% confidence	Gansu	Kongtong District, Chongxin County, Huating City
	Heilongjiang	g Aihui District
	Shaanxi	Weibin District, Jintai District, Chencang District, Fengxiang County, Long County, Qianyang County, Taibai County, Shiquan County
	Xizang	Zuogong County

Abbreviation: KBD=Kashin-Beck disease; YLDs=years lived with disability; PLAD=provincial-level administrative division.

health technicians was always negatively associated with YLD rates in both years. This negative correlation was observed in 230 counties across 10 PLADs, including Shanxi, Inner Mongolia, Jilin, Heilongjiang, Gansu, Qinghai, Sichuan, Henan, Shaanxi, and Xizang (Supplementary Table S1, available at https://weekly.chinacdc.cn/). Thus, there is a need to increase human resource allocation in primary healthcare to strengthen disease prevention and control systems.

#### **DISCUSSION**

In this study, we selected YLDs over single measures, such as prevalence, to more comprehensively reflect the population-level and societal burden of nonfatal disability associated with KBD. In addition, the use of YLDs provides a more in-depth evaluation of the disease burden among existing patients with KBD across the country.

The YLDs among patients with KBD exhibited significant spatial clustering at the county level. The

extent of YLD hotspots declined in 2023 compared to that in 2019; however, persistent hotspots remained, primarily located in 81 endemic counties in Shaanxi, Gansu, and Sichuan in the western region and 9 counties in Heilongjiang and Inner Mongolia in the northern region. The formation of these hotspots may be associated with long-standing geographic and environmental characteristics at the district and county levels. Historically, regional geographic environments have shaped unique living and dietary patterns among local populations, influencing the incidence of KBD to varying extents over time. Consequently, substantial regional disparities in KBD prevalence have emerged, contributing to the current spatial heterogeneity in the YLD rates among patients with KBD (14).

Previous studies have reported that KBD occurs in areas with lagging economic development (15). However, we found no statistically significant correlation between YLD rates and local economic levels in both 2019 and 2023. The implementation of policies such as the National Twelfth Five-Year Plan for the Prevention and Control of Endemic Diseases

TABLE 3. Descriptive statistics of OLS analysis results and GWR model parameter estimates.

Year	Variable	OLS mo	del	GWR model						
rear	variable	Coefficient	P	Max	Min	Mean	SD			
	Per capita GDP	0.060	0.299	14.950	-0.995	0.686	2.124			
2010	Per capita income	0.018	0.757	0.627	-0.303	0.638	0.219			
2019	Number of hospital beds	0.003	0.971	0.303	-0.641	0.020	0.133			
	Number of health technicians	-0.184	0.007*	1.818	-1.037	-0.150	0.244			
	Per capita GDP	-0.008	0.887	0.251	-0.335	-0.028	0.114			
2022	Per capita income	0.064	0.269	0.482	-0.204	0.012	0.140			
2023	Number of hospital beds	-0.053	0.359	0.168	-0.385	-0.082	0.153			
	Number of health technicians	-0.135	0.019*	0.295	-0.577	-0.149	0.173			

Abbreviation: SD=standard deviation; OLS=ordinary least squares; GWR=geographically weighted regression; GDP=gross domestic product.

and the Three-Year Special Action Plan for Tackling Endemic Diseases (2018–2020), which include relocation, targeted care, health poverty relief, and increased funding for disease control, may have significantly improved the economic conditions in KBD-endemic areas. Narrowing regional economic disparities, and increased investment in medical resources (e.g., hospital construction, medical equipment, and drug supply) in these regions have effectively alleviating uneven distribution of healthcare resources.

Despite this progress, our study identified a significant negative correlation between the number of health technicians and YLD rates for both 2019 and 2023. Thus, a shortage of specialized health personnel may limit patients' access to adequate treatment and rehabilitation services, thereby negatively affecting their quality of life.

Therefore, targeted interventions should be introduced to identify areas with high YLD rates and insufficient healthcare personnel. These include the recruitment of professional health technicians, tailored training programs, and optimized medical resource allocation to enhance KBD prevention and treatment in underserved areas. In addition, efforts should be made to increase the supply of medications and medical equipment to primary healthcare institutions, ensure the availability of symptomatic treatments, and ultimately improve the quality of life of patients with KBD.

Future studies could include additional metrics such as functional impairment scores (e.g., WOMAC and HAQ) and quality of life measures (e.g., SF-36) among patients with KBD to enhance the framework for evaluating the health burden of KBD and provide a

more comprehensive and systematic understanding of its impact.

This study had two main limitations. Firstly, no established studies have defined the disease-specific disability weights for patients with KBD. Therefore, disability weights for rheumatoid arthritis from the GBD 2019 study were used as proxies. Secondly, a small proportion (<5%) of cases were missing due to population movement, mortality, and urbanization and were therefore excluded from the spatial analysis. Although this proportion was minor, it was unlikely to affect the overall representativeness of the dataset substantially.

**Conflicts of interest**: No conflicts of interest.

Acknowledgments: We extend our gratitude to the disease control and prevention centers of 13 provinces (autonomous regions and municipalities) for their assistance, and we thank the patients participating in the Kashin-Beck Disease (KBD) surveillance program for their trust and cooperation.

Ethical statement: The study protocol was approved by the Ethics Committee of Harbin Medical University, with approval number (hrbmuecdc20221102). The research was conducted in accordance with the ethical guidelines and principles outlined in the Declaration of Helsinki.

**Funding:** Supported by National Key Research and Development Program of China 2022YFC2503101.

doi: 10.46234/ccdcw2025.237

<sup>\*</sup> P<0.05, denoting statistical significance.

<sup>\*</sup> Corresponding author: Jun Yu, 400049@hrbmu.edu.cn.

<sup>&</sup>lt;sup>1</sup> Institute for Kashin-Beck Disease Control and Prevention, Center for Endemic Disease Control, Chinese Center for Disease Control and Prevention, Harbin Medical University, Harbin City, Heilongjiang Province, China; <sup>2</sup> National Healthy Commission Key Laboratory of Etiology and Epidemiology (Harbin Medical University), Key Laboratory of Etiology and Epidemiology, Education Bureau of

Heilongjiang Province, Heilongjiang Provincial Laboratory of Trace Element and Human Health, Harbin Medical University, Harbin City, Heilongjiang Province, China.

Copyright © 2025 by Chinese Center for Disease Control and Prevention. All content is distributed under a Creative Commons Attribution Non Commercial License 4.0 (CC BY-NC).

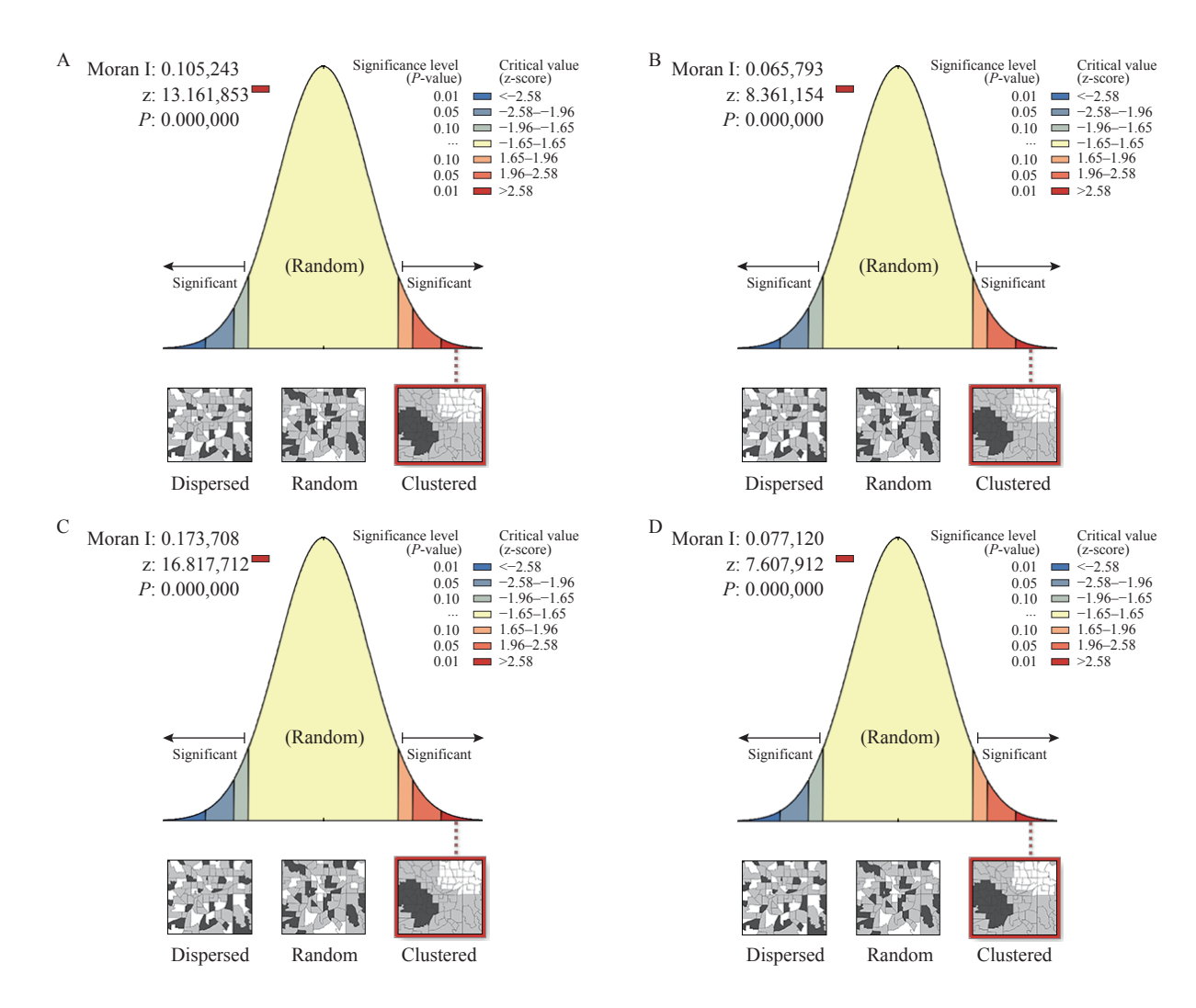
Submitted: June 22, 2025 Accepted: August 31, 2025 Issued: November 07, 2025

#### **REFERENCES**

- 1. Jiang T, Yan JN, Tan HX, Pu Z, Wang O, Liu T, et al. Prevalence of T-2 Toxin in the food and beverages of residents living in a Kashin-Beck-disease area of Qamdo, xizang. Nutrients 2024;16(10):1449. https://doi.org/10.3390/nu16101449.
- Jin ZK, Wu XY, Sun ZM, Chen M, Yang B, Dong XH, et al. Healthrelated quality of life in patients with Kashin-Beck disease is lower than in those with osteoarthritis: a cross-sectional study. J Orthop Surg Res 2023;18(1):330. https://doi.org/10.1186/s13018-023-03803-8.
- Wang J, Li RN, Wei BG, Li HR, Guo M. Spatiotemporal process and mechanism of Kashin-Beck disease regression in Xizang during 2000-2015. Acta Geogr Sin 2024;79(11):2849 – 63. https://doi.org/10. 11821/dlxb202411010.
- Cui SL, Pei JR, Jiao Z, Deng Q, Liu N, Cao YH, et al. Summary report of a national survey of Kashin-Beck disease prevalence in 2020. Chin J Endemiol 2023;42(6):488 – 92. https://doi.org/10.3760/cma.j. cn231583-20220524-00184.
- Guo LL, Wang HB, Lv FQ, Wang XH, Chen XY. Investigation and analysis of the current situation of adult Kashin-Beck disease patients in Pingliang City. Chin J Ctrl Endem Dis 2022;37(3):215-8. https://d. wanfangdata.com.cn/periodical/ChVQZXJpb2RpY2FsQ0hJMjAy NTA2MjISEnpnZGZiZnp6ejIwMjIwMzAxMxoIbW9xOHRxdTk%3 D. (In Chinese).
- 6. Cui SL, Que WJ, Jiao Z, Deng Q, Zhang XF, Cao YH, et al. Disease

- and economic burden of Kashin-Beck disease China, 2021. China CDC Wkly 2024;6(2):40 4. https://doi.org/10.46234/ccdcw2024.
- Resche-Rigon M, White IR. Multiple imputation by chained equations for systematically and sporadically missing multilevel data. Stat Methods Med Res 2018;27(6):1634 – 49. https://doi.org/10.1177/ 0962280216666564.
- Wang J, Wang XY, Li HR, Yang LS, Li YC, Kong C. Spatial distribution and determinants of health loss from Kashin-Beck disease in Bin County, Shaanxi Province, China. BMC Public Health 2021;21 (1):387. https://doi.org/10.1186/s12889-021-10407-6.
- Liu D, Wang ZL. Differential diagnosis of Kashin-Beck disease and rheumatoid arthritis. Chin J Ctrl Endem Dis 2009;24(3):195-7. https:// www.doc88.com/p-7468995693585.html. (In Chinese).
- Global Burden of Disease Collaborative Network. Global Burden of disease study 2019 (GBD 2019) Disability Weights [DB/OL]. Institute for Health Metrics and Evaluation (IHME): Seattle, DC, USA, 2020. Available online: http://ghdx.healthdata.org/record/ihme-data/gbd-2019-disability-weights.2024-01-04
- Yu SS, Pan Y, Chen QP, Liu Q, Wang J, Rui J, et al. Analysis of the epidemiological characteristics and influencing factors of tuberculosis among students in a large province of China, 2008-2018. Sci Rep 2024;14(1):20472. https://doi.org/10.1038/s41598-024-71720-9.
- 12. Wu X, Zhang JT. Exploration of spatial-temporal varying impacts on COVID-19 cumulative case in Texas using geographically weighted regression (GWR). Environ Sci Pollut Res 2021;28(32):43732 46. https://doi.org/10.1007/s11356-021-13653-8.
- 13. Ma XW. Diagnosis and empirical analysis on multicollinearity in linear regression model. J Huazhong Agric Univ (Soc Sci Ed) 2008(2):78 81,85. https://doi.org/10.3969/j.issn.1008-3456.2008.02.019.
- Guang L, Xing QJ. Analysising geography environmental factors about Keshan disease and Kashin-Beck disease. J Shanxi Norm Univ (Nat Sci Ed) 2004;18(2):81 – 6. https://doi.org/10.3969/j.issn.1009-4490.2004. 02.016
- Luo ZG, Liu YY, Han ZJ. Spatiotemporal clustering characteristics and environmental risks of Kashin-Beck disease in Gansu Province. Chin J Ctrl Endem Dis 2024;39(5):361-4,377. https://d.wanfangdata.com.cn/ periodical/zgdfbfzzz202405001. (In Chinese).

#### **SUPPLEMENTARY MATERIAL**



SUPPLEMENTARY FIGURE S1. Statistical plots of global spatial autocorrelation test results for YLDs and YLD rates among KBD patients. (A) YLDs among KBD patients in 2019; (B) YLD rates among KBD patients in 2019; (C) YLDs among KBD patients in 2023; (D) YLD rates among KBD patients in 2023.

Abbreviation: KBD=Kashin-Beck disease; YLDs=years lived with disability.

#### China CDC Weekly

SUPPLEMENTARY TABLE S1. Counties with an inverse relationship between YLDs rate and number of health technicians for patients with KBD in 2019 and 2023.

PLADs	Number of counties	Counties
Heilongjiang	57	Acheng District, Yilan County, Fangzheng County, Bayan County, Mulan County, Tonghe County, Yanshou County, Shangzhi City, Wuchang City, Meilisi Daur District, Longjiang County, Yi'an County, Gannan County, Fuyu County, Keshan County, Kedong County, Baiquan County, Jiguan District, Hengshan District, Didao District, Lishu District, Chengzihe District, Mashan District, Jidong County, Hulin City, Mishan City, Luobei County, Lingdong District, Sifangtai District, Jixian County, Raohe County, Longfeng District, Ranghulu District, Datong District, Lindian County, Jiayin County, Nancha County, Tieli City, Suburban District, Huachuan County, Tongjiang City, Fujin City, Boli County, Xi'an District, Linkou County, Suifenhe City, Hailin City, Ning'an City, Muling City, Dongning City, Xunke County, Bei'an City, Wudalianchi City, Mingshui County, Suileng County, Zhaodong City, Hailun City
Shaanxi	55	Baqiao District, Lintong District, Lantian County, Zhouzhi County, Wangyi District, Yintai District, Yaozhou District, Yijun County, Weibin District, Jintai District, Chencang District, Fengxiang County, Qishan County, Fufeng County, Mei County, Long County, Qianyang County, Linyou County, Taibai County, Sanyuan County, Jingyang County, Qian County, Liquan County, Yongshou County, Changwu County, Xunyi County, Chunhua County, Binzhou City, Linwei District, Huazhou District, Tongguan County, Heyang County, Chengcheng County, Pucheng County, Baishui County, Fuping County, Hancheng City, Baota District, Ansai District, Yanchang County, Zhidan County, Ganquan County, Fu County, Luochuan County, Yichuan County, Huanglong County, Huangling County, Yuyang District, Shenmu City, Hanbin District, Ningshan County, Shangzhou District, Luonan County, Zhen'an County, Zhashui County
Shanxi	33	Guangling County, Tunliu District, Changzi County, Wuxiang County, Qin County, Qinyuan County, Qinshui County, Yushe County, Zuoquan County, Heshun County, Wenxi County, Jishan County, Jiang County, Yuanqu County, Xia County, Pinglu County, Ruicheng County, Xiangfen County, Gu County, Anze County, Fushan County, Ji County, Xiangning County, Daning County, Xi County, Yonghe County, Pu County, Fenxi County, Huozhou City, Lishi District, Shilou County, Fangshan County, Jiaokou County
Sichuan	26	Beichuan Qiang Autonomous County, Pingwu County, Yucheng District, Hanyuan County, Shimian County, Tianquan County, Maerkang City, Wenchuan County, Mao County, Songpan County, Jiuzhaigou County, Jinchuan County, Xiaojin County, Heishui County, Rangtang County, Aba County, Ruo'ergai County, Hongyuan County, Luding County, Danba County, Daofu County, Ganzi County, Xinlong County, Dege County, Seda County, Mianning County
Jilin	25	Shuangyang District, Yushu City, Longtan District, Chuanying District, Fengman District, Yongji County, Jiaohe City, Huadian City, Shulan City, Panshi City, Yitong Manchu Autonomous County, Xi'ar District, Fusong County, Jingyu County, Qian Gorlos Mongol Autonomous County, Changling County, Qianguo County, Yanji City, Tumen City, Dunhua City, Hunchun City, Longjing City, Helong City, Wangqing County, Antu County
Gansu	22	Qinzhou District, Maiji District, Qingshui County, Qin'an County, Wushan County, Zhangjiachuan Hui Autonomous County, Kongtong District, Zhuanglang County, Huating City, Huan County, Huachi County, Heshui County, Zhengning County, Weiyuan County, Zhang County, Min County, Dangchang County, Li County, Kangle County, Hezheng County, Zhuoni County, Luqu County
Henan	5	Luoning County, Shanzhou District, Mianchi County, Lushi County, Lingbao City
Inner Mongolia	3	Uxin Banner, Zhalaite Banner, Tuquan County
Qinghai	3	Guide County, Xinghai County, Banma County
Xizang	1	Xietongmen County

Abbreviation: KBD=Kashin–Beck disease; YLDs=years lived with disability; PLAD=provincial-level administrative division.

#### **Preplanned Studies**

# Development of a Landscape Pattern Health Index and Association with Stroke Mortality Using GWQS Regression — Ningbo City, Zhejiang Province, China, 2001–2023

Qinsheng Kong<sup>1</sup>; Jing Huang<sup>1</sup>; Tianfeng He<sup>2,#</sup>; Guoxing Li<sup>1,3,#</sup>

#### **Summary**

#### What is already known about this topic?

Urban landscape patterns influence population health and are traditionally measured using landscape indices. However, current indices suffer from a single-dimensional focus, multicollinearity, and limited health relevance.

#### What is added by this report?

Using a two-stage Generalized Weighted Quantile Sum (GWQS) regression, we developed a Landscape Pattern Health Index (LPHI), integrating composition/configuration metrics. This index revealed seasonal protective/hazard effects and represents a holistic tool for assessing urban landscape health impacts.

### What are the implications for public health practice?

The LPHI identifies high-risk areas and seasonal priorities, thereby guiding targeted interventions to mitigate health risks through landscape optimization.

#### **ABSTRACT**

**Introduction:** Urban landscape patterns impact population health; however, traditional indices are limited by single-dimensional focus, multicollinearity, and weak health relevance. Developing a holistic Landscape Pattern Health Index (LPHI) is critical for planning healthy cities.

Methods: Using data from Ningbo (China), this study integrated 2001–2023 land use data (reclassified into 7 types) and 2009–2016 street-level stroke mortality data. A two-stage Generalized Weighted Quantile Sum (GWQS) regression addressed the temporal data discrepancy, first deriving weights from 2009–2016 health data, then calculating the LPHI for the full 2001–2023 period. Quasi-Poisson regression was used to validate the association between the LPHI and stroke mortality.

Results: An interquartile-range increase in the Protective Composite Index reduced stroke mortality by 20% (warm seasons) and 22% (cold seasons), while the Hazard Composite Index increased risk by 29% (warm) and 20% (cold). The LPHI demonstrated significant associations with stroke mortality, with the Protective Composite Index reducing risk and the Hazard Composite Index increasing it across both seasons.

**Conclusion:** The study suggests that the LPHI can serve as a bridge between landscape ecology and public health, with the potential to identify high-risk areas and seasonal priorities. This approach could guide targeted interventions through landscape optimization, supporting evidence-based healthy urban planning.

Urban landscape patterns influence population health through the spatial distribution of green spaces (1) and water bodies (2) that mitigate pollution and promote physical activity, whereas industrial land use increases cardiovascular risks (3). Configurations such as high edge density in green spaces may facilitate physical activity and social cohesion, whereas impervious surface complexity may exacerbate urban heat island effects and pollutant accumulation, indirectly influencing stroke risk via microclimatic and physiological pathways. Landscape patterns are typically quantified using indices; however, existing indices often focus on a single dimension and face challenges, such as multicollinearity and limited relevance. Inspired by the Air Quality Health Index (AQHI)(4), we developed the Landscape Pattern Health Index (LPHI) that integrates statistical robustness, practical utility, and public health guidance, all critical for Healthy City initiatives.

In environmental health, generalized weighted quantile sum (GWQS) regression models can assess the health impacts of exposure to mixed air pollutants and chemicals, effectively reducing collinearity among components. Unlike dimension-reduction techniques such as Principal Component Analysis (PCA), which create latent factors not tied directly to health outcomes, GWQS regression derives component weights explicitly from associations with health, generating more interpretable and health-relevant composite indices, reducing multicollinearity among correlated indicators, enabling integrated health-oriented indices creation, and advancing evidence-based strategies for urban landscape optimization. Based on data from Ningbo, we employed GWQS regression to construct an LPHI, offering a tool for planning healthy cities.

We collected annual land use data (500m resolution) the MCD12O1 land cover dataset (https://earthexplorer.usgs.gov/) from 2001-2023, reclassified into seven major categories: impervious surface, grassland, cropland, bare land, wetland, waterbody, and forest/shrubland. Stroke was chosen as the outcome as it is the leading cause of death in China (5), and existing literature suggests its susceptibility to environmental influences mediated by landscape patterns, including air quality, temperature extremes, and opportunities for physical activity (6). Daily streetlevel stroke mortality data from the Ningbo CDC were aggregated into annual counts at the street-unit level to achieve spatiotemporal alignment with landscape and covariate data. However, owing to data availability, these data were sourced from 2009-2016. To reconcile the temporal mismatch between the landscape (2001-2023) and health (2009-2016) data, a twoanalytical approach employed stage was (Supplementary Material, available at https://weekly. chinacdc.cn/). Briefly, Stage 1 established metrichealth associations and derived weights using 2009-2016 data; Stage 2 applied these weights to calculate the LPHI for the 2001-2023 period. Meteorological and pollutant (e.g., PM2.5) data were sourced from the China Meteorological Forcing Dataset (7) and China High Air Pollutants Datasets (8), respectively. Data on key meteorological and air quality confounders were incorporated as covariates in subsequent regression models to isolate independent associations between landscape patterns and stroke risk, following adjustment to a 1 km resolution using bilinear interpolation. Nighttime-light data (500m resolution) were applied to reflect economic disparities across streets. Summary statistics for stroke deaths, pollutant concentrations, meteorological factors, and nighttime light intensity across street-units during warm and cold seasons (2009–2016) are provided in Supplementary Table S1.

For urban landscape patterns, we selected six indices: one composition metric (Percentage of Landscape, PLAND) and five configuration metrics [patch density (PD), largest patch index (LPI), edge density (ED), mean shape index (SHAPE\_MN), and aggregation index (AI)]. The selection was based on the rationale that these metrics quantify fundamental spatial characteristics, such as the abundance, size, shape, and connectivity of landscape elements, which are theorized to influence environmental exposure (e.g., pollution and heat) and health-promoting opportunities (e.g., physical activity), thereby constituting plausible pathways to population health.

The analysis applied a two-stage GWQS regression. First, landscape metrics were scaled into quartiles, and bootstrap sampling (100 iterations) was applied to estimate weights linking metrics to health outcomes, generating a land use-specific health index classified as protective or hazardous based on their association direction. Second, metrics sharing consistent protective or hazardous associations were aggregated via GWQS to derive composite LPHIs (protective and hazardous), thereby enabling a holistic assessment of the health impacts of landscape patterns. To validate the effectiveness of the constructed LPHIs, a separate quasi-Poisson regression was applied, modeling stroke mortality as a function of the LPHI scores, while including the same set of covariates for adjustment. Statistical analyses were conducted using R software (version 4.2.3; R Core Team, R Foundation for Statistical Computing, Vienna, Austria).

Supplementary Table S2 (available at https://weekly.chinacdc.cn/) details the health indices constructed for each land-use type, revealing harmful associations between stroke mortality and indices for impervious surfaces and bare land. Protective associations were identified for grassland, cropland, wetland, waterbody, and forest/shrubland. Spatial configuration metrics (e.g., PD) outweighed landscape composition by weighting the components of health indices, underscoring their predominant influence on health (Supplementary Table S3, available at https://weekly.chinacdc.cn/).

Figure 1 shows the constituent weights of protective and hazardous composite indices. The warm-season Protective Composite Index prioritized grassland-PD (20.04%), grassland-AI (17.81%), and forest/shrubland-LPI (15.88%), emphasizing the importance of fragmented green spaces. In contrast,

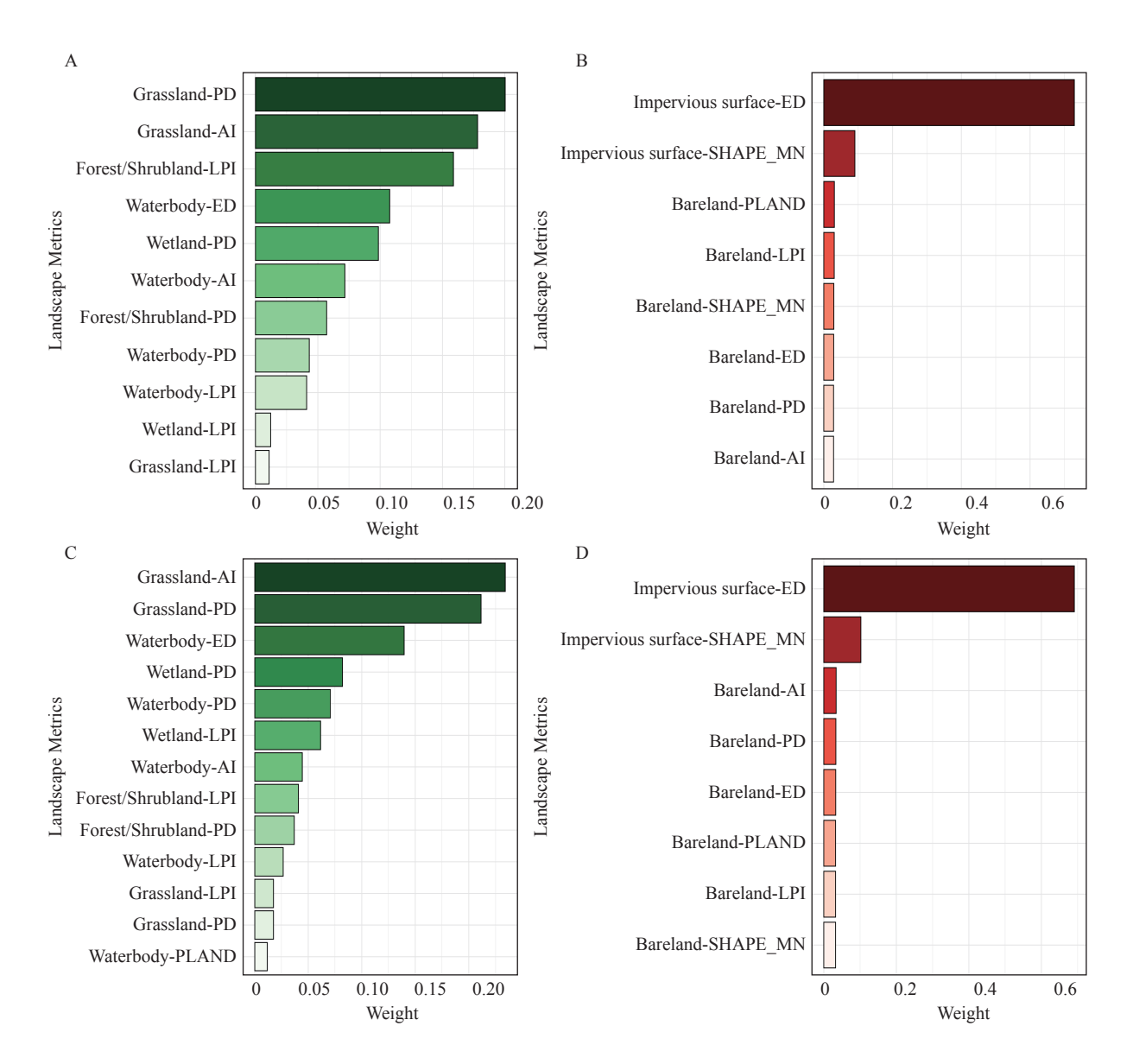


FIGURE 1. Weights of the constituent factors of the season-specific LPHI.

Note: Weights represent the relative contribution of each landscape metric derived from the GWQS regression for the (A) Protective Composite Index (Warm); (B) Hazard Composite Index (Cold); (C) Protective Composite Index (Warm); (D) Hazard Composite Index (Cold). The sum of the weights for each composite index is 100%. The metrics are sorted in descending order of their weights.

Abbreviation: Grassland-PD=Grassland Patch Density; Grassland-Al=Grassland Aggregation Index; Forest/Shrubland-LPI=Forest/Shrubland Largest Patch Index; Waterbody-ED=Waterbody Edge Density; Wetland-PD=Wetland Patch Density; Forest/Shrubland-PD=Forest/Shrubland Patch Density; Waterbody-PD=Waterbody Patch Density; Waterbody-LPI=Waterbody Largest Patch Index; Wetland-LPI=Wetland Largest Patch Index; Grassland-LPI=Grassland Largest Patch Index; Waterbody-PLAND=Waterbody Percentage of Landscape; Impervious surface-ED=Impervious Surface Edge Density; Impervious surface-SHAPE\_MN=Impervious Surface Mean Shape Index; Bareland-PLAND=Bareland Percentage of Landscape; Bareland-LPI=Bareland Largest Patch Index; Bareland-SHAPE\_MN=Bareland Mean Shape Index; Bareland-ED=Bareland Edge Density; Bareland-PD=Bareland Patch Density; Bareland-AI=Bareland Aggregation Index.

the cold-season Protective Composite Index relied on grassland-AI (23.42%), grassland-PD (21.14%), and waterbody-ED (13.96%), reflecting enhanced natural vegetation and water connectivity during colder months. The Hazard Composite Index was overwhelmingly driven by impervious surface ED

(warm: 72.86%; cold: 69.07%) and SHAPE\_MN (warm: 9.04%; cold: 10.20%), indicating that irregular impervious patches posed a year-round risk.

For the composite LPHIs (Table 1), the Hazard Composite Index had higher mean values in warm (1.16, *IQR*=1.64) than cold (1.13, *IQR*=1.58) seasons,

TABLE 1. Descriptive statistics of the constructed LPHI (2001–2023) and Percentage change (mean and 95% posterior intervals) in stroke mortality associated with an interquartile range (*IQR*) increase in LPHI.

0	1 800		Desc	riptive Statis	Cároko mortality (M)	P		
Seasons	LPHI	Mean	IQR	Median	Min	Max	Stroke mortality (%)	P
Marm	Protective Composite Index	0.90	0.48	0.92	0.01	1.66	-20 (-26, -13)	<0.001
Warm	Hazard Composite Index	1.16	1.64	1.46	0.00	2.47	+29 (+19, +40)	<0.001
Cold	Protective Composite Index	0.94	0.46	0.92	0.02	2.03	-22 (-28, -16)	<0.001
Cold	Hazard Composite Index	1.13	1.58	1.38	0.00	2.41	+20 (+11, +29)	<0.001

Note: '+' indicates a percentage increase in stroke mortality associated with an IQR increase in LPHI, whereas '-' represents a percentage decrease linked to an IQR increase in LPHI.

Abbreviation: LPHI=Landscape Pattern Health Index; IQR=interguartile range.

with extreme ranges spanning 0.00-2.47. The Protective Composite Index exhibited similar means across seasons (warm: 0.90; cold: 0.94), but a higher maximum in cold seasons (2.03 compared to 1.66), suggesting a stronger protective potential of natural landscapes in winter. Regression results confirmed the validity of the LPHI: each IQR increase in the Protective Composite Index reduced the stroke mortality risk by 20% (13%-26%) in warm seasons and 22% (16%-28%) in cold seasons. Conversely, the Hazard Composite Index increased risk by 29% (19%-40%) and 20% (11%-29%), respectively (all P < 0.001). Together, these findings demonstrate a robust association between the LPHI and stroke mortality, supporting its validity as a framework for assessing the health effects of urban landscape patterns.

#### **DISCUSSION**

the associations between constructed for individual land use types and stroke mortality, grassland, cropland, wetland, waterbodies, and forest/shrubland reduced risks in both seasons, whereas impervious surfaces and bare land increased risks. This aligns with the known benefits of green (1) and blue spaces (2). Vegetated areas are likely to mitigate the risk through pollutant absorption, microclimate regulation, and stress reduction. Although no direct studies have linked impervious surfaces or bare land to stroke mortality, built environment density is positively correlated with stroke risk (6). Impervious surfaces, particularly those with complex shapes and extensive edges, intensify the urban heat island effect (9). This can elevate stroke risk through temperature-dependent pathways such as exacerbated heat stress, which reduces cerebral perfusion in warm seasons and heightens cold-induced hemodynamic instability in cold seasons (10). Barelands lacking vegetation may similarly experience

extreme temperature exposure.

The LPHI, developed through GWQS regression, addresses the key limitations of traditional indices, including single-dimensional focus, multicollinearity, and weak health linkages, by systematically integrating both landscape composition (e.g., impervious surfaces and green space coverage) and configuration metrics (e.g., patch density and aggregation). Its dual protective-hazardous index design provides a holistic framework to assess both risk-mitigating and riskamplifying landscape features, revealing that the protective effects of grasslands and water bodies depend on features such as fragmented green spaces (facilitating activity) in warm seasons, whereas hazardous risks from impervious surfaces relate to edge complexity, whose irregular configurations may exacerbate the heat island effect or pollutant accumulation, thereby increasing the risk of stroke. By prioritizing metrics with strong health associations, the LPHI bridges landscape ecology and public health and offers a robust tool for quantifying the impact of urban forms on health outcomes.

A key innovation of this study is the development of the LPHI via GWQS regression. Our findings suggest that this approach can translate complex landscape patterns into a composite tool with potential public health utility. The significant associations observed support the idea that the LPHI can holistically assess health risks and benefits from urban landscapes, which could enable better prioritization of interventions, such as enhancing green space connectivity or managing impervious surface expansion, to mitigate population health risks.

However, the LPHI framework has several limitations. Validated in Ningbo, its generalizability may face challenges owing to varying local land use, climate, and health contexts. The 500m resolution remote sensing data may overlook microscale features with neighborhood-level health impacts, such as small

park accessibility. Socioeconomic factors, such as income inequality, indirectly inferred from nighttime light data, should be explicitly integrated. Relying solely on stroke mortality restricted the study's scope. Stroke, a chronic disease with acute manifestations, requires the precise alignment of long-term landscape exposures (e.g., pre-2009 data gaps) with acute triggers (partially addressed here). Different diseases (e.g., asthma and tumors) exhibit distinct environmental sensitivities (e.g., tumors to industrial pollution), necessitating multi-disease validation. Static residential assumptions ignore migration (e.g., rural-to-urban moves) and biased associations for chronic diseases, such as stroke, influenced by past exposure. These gaps highlight the need for higher-resolution data, explicit socioeconomic indicators, multiple diseases, and longitudinal analyses to enhance LPHI's utility.

Despite these limitations, the LPHI bridges landscape ecology and public health, offering a scalable tool for healthy urban planning. In the big data era, real-time sensing (e.g., Sentinel-2) and machine learning may be integrated to predict landscape health risks (e.g., impervious surface growth) and guide smart interventions, such as green corridor prioritization. This aligns with the need to deepen LPHI public health applications using data-driven insights for enhanced risk control. Given the burden of stroke and environmentally sensitive diseases, integrating LPHI into policies fosters proactive place-based strategies. This ensures that landscape design matches health priorities, supports sustainability and population health while leveraging technology for precision public health.

**Conflicts of interest**: No conflicts of interest.

Ethical Statement: This study, which involved human subjects, was conducted in accordance with the Declaration of Helsinki, the International Ethical Guidelines for Biomedical Research Involving Human Subjects, and relevant Chinese regulations, including the "Ethical Review Measures for Life Sciences and Medical Research Involving Humans." The study protocol was reviewed and approved by the Biomedical Ethics Committee of the Peking University (approval number: PURB-TYS2025175).

**Funding:** Supported by the Noncommunicable Chronic Diseases-National Science and Technology

Major Project (2024ZD0531603).

doi: 10.46234/ccdcw2025.239

\* Corresponding authors: Guoxing Li: liguoxing@bjmu.edu.cn; Tianfeng He: hetf@nbcdc.org.cn.

Copyright © 2025 by Chinese Center for Disease Control and Prevention. All content is distributed under a Creative Commons Attribution Non Commercial License 4.0 (CC BY-NC).

Submitted: April 23, 2025 Accepted: October 24, 2025 Issued: November 07, 2025

#### REFERENCES

- 1. Shen YS, Lung SCC. Can green structure reduce the mortality of cardiovascular diseases? Sci Total Environ 2016;566-567:1159-67. http://dx.doi.org/10.1016/j.scitotenv.2016.05.159.
- Kasdagli MI, Katsouyanni K, de Hoogh K, Zafeiratou S, Dimakopoulou K, Samoli E. Associations between exposure to blue spaces and natural and cause-specific mortality in Greece: an ecological study. Int J Hyg Environ Health 2023;249:114137. https://doi.org/10. 1016/j.ijheh.2023.114137.
- Shi JX, Dong SX. Study on the influence of built environmental factors on cardiovascular diseases in middle-aged and elderly people. Mod Prev Med 2024;51(9):1586 – 90. https://doi.org/10.20043/j.cnki.MPM. 202312457.
- Sun QH, Zhu HH, Shi WY, Zhong Y, Zhang YJ, Li TT. Development of the national air quality health index - China, 2013-2018. China CDC Wkly 2021;3(4):61 - 4. https://doi.org/10.46234/ccdcw2021. 011
- Tu WJ, Wang LD. China stroke surveillance report 2021. Mil Med Res 2023;10(1):33. https://doi.org/10.1186/s40779-023-00463-x.
- Xie B, Zheng YL, Li ZG, An ZH. Influence of urban high-density living environment on stroke risk: a case study of Wuhan. City Plann Rev 2021;45(5):30 – 9. https://doi.org/10.11819/cpr20210504a.
- He J, Yang K, Tang WJ, Lu H, Qin J, Chen YY, et al. The first highresolution meteorological forcing dataset for land process studies over China. Sci Data 2020;7(1):25. https://doi.org/10.1038/s41597-020-0369-y.
- Wei J, Li ZQ, Lyapustin A, Wang J, Dubovik O, Schwartz J, et al. First close insight into global daily gapless 1 km PM<sub>2.5</sub> pollution, variability, and health impact. Nat Commun 2023;14(1):8349. https://doi.org/10. 1038/s41467-023-43862-3.
- 9. Liu YL, Jiang JP, Wu F, Cen MY. Analysis of the regulating effect of ecological land on urban thermal environment in Dongguan City. Theor Res Urban Constr 2024;10:36-9. http://dx.doi.org/10.19569/j.cnki.cn119313/tu.202410012. (In Chinese).
- Avila-Palencia I, Rodríguez DA, Miranda JJ, Moore K, Gouveia N, Moran MR, et al. Associations of urban environment features with hypertension and blood pressure across 230 Latin American cities. Environ Health Perspect 2022;130(2):27010. https://doi.org/10.1289/ ehp7870.

<sup>&</sup>lt;sup>1</sup> Health Science Center, Peking University, Beijing, China; <sup>2</sup> Ningbo Municipal Center for Disease Control and Prevention, Ningbo City, Zhejiang Province, China; <sup>3</sup> Environmental Research Group, School of Public Health, Imperial College London, London, United Kingdom.

#### **SUPPLEMENTARY MATERIAL**

#### TEMPORAL SCOPE OF HEALTH OUTCOME AND LANDSCAPE DATA.

Due to data availability constraints, the health outcome data (stroke mortality) used in this study were sourced from 2009-2016, while the landscape pattern indices were derived from land use data collected from 2001-2023. To account for this temporal discrepancy in our analysis, a two-step approach was employed, as outlined below:

#### **Step 1: Establishing Weights of Landscape Indices**

For the 2009–2016 period, we aimed to establish the weights of landscape indices associated with health outcomes. First, we standardized the landscape indices into 4 quantiles. Using a bootstrap sampling method with 100 resamples and maximum likelihood estimation, we estimated the weights,  $w_i$ , of each landscape index,  $q_i$  (i=1-c, where c=6), associated with the health outcome. This was done by solving the equation:

$$E(\mathbf{u}) = \alpha + \beta \times \left(\sum_{i=1}^{c} \mathbf{w}_{i} \mathbf{q}_{i}\right) + \mathbf{z}^{T} \boldsymbol{\varphi}$$

A detailed explanation of GWQS regression model parameters is provided below:

E(u): The expected number of deaths from stroke. This is the value that the model ultimately aims to predict, reflecting the theoretically expected number of stroke deaths based on landscape indices and other covariates.

 $\alpha$ : The intercept term. When all landscape index variables (q<sub>i</sub>) are 0 and other covariates (z) are also 0,  $\alpha$  represents the expected number of stroke deaths, serving as a baseline value for the model.

 $w_i$ : The weight of the landscape index  $q_i$ . Its value range is  $0 \le w_i \le 1$  and  $\sum_{i=1}^{c} w_i = 1$ . These weights determined the relative importance of each landscape index in comprehensively influencing stroke mortality.

 $q_i$ : Landscape indices. Here, i = 1-c (c=6), representing different quantitative indicators of landscape patterns such as PLAND and PD. They participated in the model calculation after being standardized into four quantiles.

β: The regression coefficient of the weighted index  $(\sum_{i=1}^{c} w_i q_i)$ . This was used to measure the degree of influence of the weighted comprehensive value of the landscape indices on the expected number of stroke deaths. Its significance in influencing the results was determined using a significance test (P < 0.05).

z: A row vector of other covariates that need to be adjusted, such as  $PM_{2.5}$ , relative humidity, economic development level, and other factors. The superscript T in  $z^T$  denotes the transpose operation, converting this row vector into a column vector for proper matrix multiplication with the coefficient vector  $\varphi$ .

 $\phi$ : The regression coefficient column vector for the covariates z, reflecting the degree of influence of each corresponding covariate on the expected number of stroke deaths.

The model was subject to the constraints  $\sum_{i=1}^{c} w_i = 1$  and  $0 \le w_i \le 1$ . For each bootstrap sample, we estimated the model parameters  $(\beta, w_i)$ , and evaluated the significance of the landscape index quantile weight  $w_i$  based on the significance of the regression coefficient  $\beta$  (P < 0.05). We then averaged the results from the significant bootstrap

SUPPLEMENTARY TABLE S1. Summary statistics on stroke deaths, pollutant concentrations, meteorological factors and nighttime light intensity across street-units in Ningbo during warm and cold seasons (2009–2016).

lu di a stava		W	arm Se	asons		-	Cold Seasons						
Indicators	Total count	Mean	SD	Median	Min	Max	Total count	Mean	SD	Median	Min	Max	
Stroke Deaths/n	18,331	0.10	0.32	0	0	6	25201	0.14	0.39	0	0	5	
Air pollutants													
$PM_{2.5}/(\mu g/m^3)$		31.5	13.43	28.95	4.27	116.71		56.71	27.25	50.63	8.96	450.59	
$NO_2/(\mu g/m^3)$		27.52	9.80	26.76	4.92	85.67		47.97	15.40	47.02	7.24	134.47	
Meteorology													
Daily mean temperature/ ${}^\circ\!{\rm C}$		25.22	3.95	25.55	9.25	35.58		8.75	4.97	8.33	-8.22	24.09	
Relative humidity/%		77.77	10.84	78.39	30.44	100.00		72.38	14.75	73.32	12.15	100.00	
Wind speed/(m/s)		2.40	1.16	2.17	0.22	19.49		2.43	1.13	2.23	0.08	10.20	
NTL/(nWcm <sup>-2</sup> sr <sup>-1</sup> )		8.39	12.36	2.69	0.00	68.24		8.39	12.36	2.69	0.00	68.24	

SUPPLEMENTARY TABLE S2. Descriptive statistics of the constructed health index (2001–2023) for each land use type and their direction of association with stroke mortality.

		Warm Seasons								Cold Seasons						
Index	Descriptive Statistics					- - RR (95% CI)		<b>Descriptive Statistics</b>				RR (95% CI)	_			
	Mean	IQR	Median	Min	Max	KK (95% CI)	P	Mean	IQR	Median	Min	Max	KK (95% CI)	<i>P</i>		
Impervious surface	1.49	2.89	1.96	0.00	3.00	1.13 (1.08,1.18)	<0.001	1.48	2.70	1.89	0.00	3.00	1.09(1.04,1.14)	<0.001		
Grassland	1.31	0.52	1.25	0.00	2.87	0.74 (0.68,0.82)	<0.001	1.29	0.56	1.21	0.00	2.83	0.75(0.69,0.82)	<0.001		
Cropland	1.55	1.97	1.96	0.00	3.00	0.93 (0.89,0.97)	0.002	1.55	1.97	1.97	0.00	3.00	0.91(0.87,0.95)	<0.001		
Bareland	1.50	1.22	1.47	0.00	3.00	1.10 (1.03,1.18)	0.007	1.43	1.14	1.24	0.00	3.00	1.11(1.03,1.18)	0.004		
Wetland	1.63	1.41	1.66	0.00	3.00	0.90 (0.84,0.97)	0.005	1.64	1.48	1.66	0.00	3.00	0.89(0.83,0.95)	0.001		
Waterbody	1.44	0.76	1.48	0.00	2.52	0.78 (0.71,0.87)	<0.001	1.44	0.79	1.48	0.00	2.58	0.80(0.73,0.88)	<0.001		
Forest/Shrubland	1.45	1.24	1.44	0.00	3.00	0.86 (0.81,0.91)	<0.001	1.44	1.40	1.40	0.00	2.99	0.88(0.83,0.94)	<0.001		

Note: RR (95% CI) >1 indicates a harmful association with health outcomes, whereas RR (95% CI) <1 suggests a protective association. Abbreviation: CI=confidence interval; RR=relative risk.

SUPPLEMENTARY TABLE S3. Weights of the constituent factors of the season-specific health index for each land use type (%).

		Wa	rm Sea	sons (%	6)		Cold Seasons (%)						
Index	Landscape Composition			Spa Configu			Landscape Composition	Spatial Configuration					
	PLAND	ΑI	ED	LPI	PD	SHAPE_MN	PLAND	ΑI	ED	LPI	PD	SHAPE_MN	
Impervious surface	0.07	0.22	97.77	0.09	0.08	1.78	0.03	0.38	93.99	0.06	0.14	5.41	
Grassland	0.09	49.13	0.05	6.83	41.76	2.14	0.07	51.82	0.06	7.13	37.74	3.17	
Cropland	0.03	0.70	0.03	1.24	97.92	0.08	0.04	0.93	0.04	0.60	98.32	0.06	
Bareland	22.45	74.77	0.59	0.07	0.93	1.17	13.77	80.80	0.24	0.03	0.47	4.69	
Wetland	1.66	3.67	8.31	26.74	59.60	0.01	1.76	0.65	6.70	33.41	57.47	0.02	
Waterbody	0.02	21.21	1.19	26.34	48.32	2.91	0.05	13.35	0.14	32.62	46.21	7.64	
orest/Shrubland	0.02	0.09	0.02	43.38	56.02	0.47	0.05	0.72	0.04	38.12	59.99	1.07	

Abbreviation: PLAND=Percentage of Landscape; Al= Aggregation Index; ED=Edge Density; LPI= Largest Patch Index; PD= Patch Density; SHAPE MN= Mean Shape Index

samples to obtain the final weights for each index.

#### Step 2: Calculating the Landscape Pattern Health Index (LPHI)

In the second step, using the weights obtained from the first-step analysis, we calculated the Landscape Pattern Health Index (LPHI) for the 2001-2023 period. Specifically, for the 2001-2023 landscape data, we first restandardized the landscape indices into four quantiles and then utilized the weighted index formula WQS=  $\sum_{i=1}^c \bar{w_i} q_i$  for the calculation, WQS: weighted quantile sum. By separating the analysis into these two steps, we were able to effectively utilize the available data and establish a comprehensive understanding of the relationship between landscape patterns and health outcomes, despite differences in their temporal scopes.

#### **Youth Editorial Board**

**Director** Lei Zhou

Vice Directors Jue Liu Tiantian Li Tianmu Chen

**Members of Youth Editorial Board** 

Jingwen Ai Li Bai Yuhai Bi Yunlong Cao Gong Cheng Liangliang Cui Meng Gao Jie Gong Yuehua Hu Xiang Huo Jia Huang Xiaolin Jiang Yu Ju Min Kang Huihui Kong Lingcai Kong Shengjie Lai Fangfang Li Jingxin Li **Huigang Liang** Di Liu Jun Liu Li Liu Yang Liu Chao Ma Yang Pan Zhixing Peng Menbao Qian Tian Qin Shuhui Song Kun Su Song Tang Bin Wang Jingyuan Wang Linghang Wang Qihui Wang Feixue Wei Xiaoli Wang Xin Wang Yongyue Wei Zhiqiang Wu Meng Xiao Tian Xiao Wuxiang Xie Lei Xu Lin Yang Canging Yu Lin Zeng Yi Zhang Yang Zhao Hong Zhou

Indexed by Science Citation Index Expanded (SCIE), Social Sciences Citation Index (SSCI), PubMed Central (PMC), Scopus, Chinese Scientific and Technical Papers and Citations, and Chinese Science Citation Database (CSCD)

#### Copyright © 2025 by Chinese Center for Disease Control and Prevention

Under the terms of the Creative Commons Attribution-Non Commercial License 4.0 (CC BY-NC), it is permissible to download, share, remix, transform, and build upon the work provided it is properly cited. The work cannot be used commercially without permission from the journal. References to non-China-CDC sites on the Internet are provided as a service to CCDC Weekly readers and do not constitute or imply endorsement of these organizations or their programs by China CDC or National Health Commission of the People's Republic of China. China CDC is not responsible for the content of non-China-CDC sites.

The inauguration of *China CDC Weekly* is in part supported by Project for Enhancing International Impact of China STM Journals Category D (PIIJ2-D-04-(2018)) of China Association for Science and Technology (CAST).



Vol. 7 No. 45 Nov. 7, 2025

#### Responsible Authority

National Disease Control and Prevention Administration

#### **Sponsor**

Chinese Center for Disease Control and Prevention

#### **Editing and Publishing**

China CDC Weekly Editorial Office No.155 Changbai Road, Changping District, Beijing, China Tel: 86-10-63150501, 63150701 Email: weekly@chinacdc.cn

#### **CSSN**

ISSN 2096-7071 (Print) ISSN 2096-3101 (Online) CN 10-1629/R1